THE UNIVERSITY OF QUEENSLAND
AUSTRALIA

MINE4123:
MINING RESEARCH PROJECT II

FINAL THESIS SUBMISSION:
AN INVESTIGATION OF THE SELF-HEATING PROPERTIES OF HEAT-AFFECTED COAL

Commissioned By: Basil Beamish

Date of Submission: 6th November 2016

Submitted By: Tim O'Neill

UQ Supervisor: Basil Beamish

Industry Supervisor: Jan Theiler

ABSTRACT

Heat-affected coal is formed through the thermal metamorphosis of coal *in situ* due to contact with or proximity to an igneous intrusion. This transformation results in a change to the self-heating properties of the coal. Coal self-heating can lead to the occurrence of spontaneous combustion. It is therefore important to understand how the self-heating properties change in order to adequately develop a Principal Mining Hazard Management Plan (PMHMP) which appropriately addresses spontaneous combustion risks.

The major aim in undertaking the project was to determine whether heat-affected coal is more or less prone to self-heating in comparison with normal coal. Further objectives included kinetically analysing the self-heating, and investigating how PMHMPs would be affected by the results.

Samples of both heat-affected and normal coal were tested for their propensity to self-heat using the standardised R_{70} method. This method involves placing the sample in an adiabatic oven at 40 °C and allowing oxidation to occur by passing a fixed rate of oxygen through the sample. The temperature is logged as self-heating occurs, and the average rate of temperature rise from 40 °C to 70 °C yields the R_{70} value. Samples of coal heat-affected to varying degrees, a normal sample from the same seam, and normal samples of various ranks from other sites were tested.

Initial comparisons between the heat-affected coal and normal coal from the same seam indicated that the heat-affected coal was much less prone to self-heating. However, when the heat-affected coal was compared to normal coal of a similar rank, the normal coal appeared to be less prone to self-heating. The root causes of these observations were attributed to physical and chemical changes in the heat-affected coal. Kinetic analysis also showed that coal self-heating has a low temperature, non-Arrhenius component.

As a result of this study, it is suggested that the presence of heat-affected coal be accounted for to avoid over or under-managing the risk of spontaneous combustion. Further investigation into the gases emitted as heat-affected coal self-heats is also recommended in order to verify the accuracy of current monitoring techniques.

CONTENTS

LIST OF FIGURES

LIST OF TABLES

1 INTRODUCTION

1.1 PROBLEM DEFINITION

The relationship between heat-affected coal, being coal that has been thermally metamorphosed through contact with an igneous intrusion, and the resulting effects on the self-heating propensity of the coal has not been adequately investigated. This research project will attempt to expand the understanding of this relationship, in order to determine whether heat-affected coal has a higher or lower self-heating propensity than normal coal.

1.2 AIMS AND OBJECTIVES

The main aim of this project is to analyse and quantify the differences in self-heating rates between heat-affected and normal coal. The specific objectives to be met during the project include:

- Identifying and analysing the processes by which heat-affected coal is formed;
- Identifying both physical and chemical properties of coal that is heat-affected;
- The collection, analysis and comparison of self-heating rate data for both heat-affected and normal coal;
- Kinetic analysis of self-heating rate data; and
- Investigation of impacts on Principal Mining Hazard Management Plans where heat-affected coal is encountered.

1.3 SCOPE

The scope of this project includes:

- Analysing the difference in physical and chemical properties between heat-affected and normal coal, such that these properties can be used to identify heat-affected coal;
- The use of the self-heating rate index (R_{70}) in order to quantify the self-heating propensity of the different coal samples;
- A comparative analysis between the self-heating propensity of heat-affected and normal coal samples; and
- A kinetic analysis in order to understand the self-heating rate of reaction behaviour.

1.4 SIGNIFICANCE AND RELEVANCE OF PROJECT

Understanding and predicting the self-heating behaviour of coal is an important aspect of the development of a Principal Mining Hazard Management Plan (PMHMP) for spontaneous combustion. With a greater understanding of the differences in self-heating due to heat-affected coal, more appropriate hazard management plans can be developed, and the overall risk of spontaneous combustion events occurring at sites with significant occurrences of heat-affected coal can be reduced.

This is important to industry, as the occurrence of spontaneous combustion poses a major health and safety risk, as well as a major economic risk with the site downtime in order to deal with the issue and the potential for permanent closure of the site. There is also the risk of a spontaneous combustion event being an ignition source for an underground mine explosion.

2 HEAT-AFFECTED COAL

2.1 FORMATION OF HEAT-AFFECTED COAL

Heat-affected coal is coal that has been thermally altered due to contact metamorphosis with igneous intrusions. Also known as natural coke, geological coke, cinder and jhama (Kwiecinska and Peterson, 2004; Singh, Sharma and Singh, 2008), heat-affected coal is formed due to exposure to the high temperatures associated with an igneous intrusion, occurring as either a dyke or a sill. Dykes are intrusions which are more extensive vertically, which may penetrate the predominantly horizontal coal strata. Sills are more extensive horizontally, which may generally form sheets either above, below or within the coal strata. Figure 1 illustrates a hypothetical schematic of the effects of igneous intrusions on coal seams.

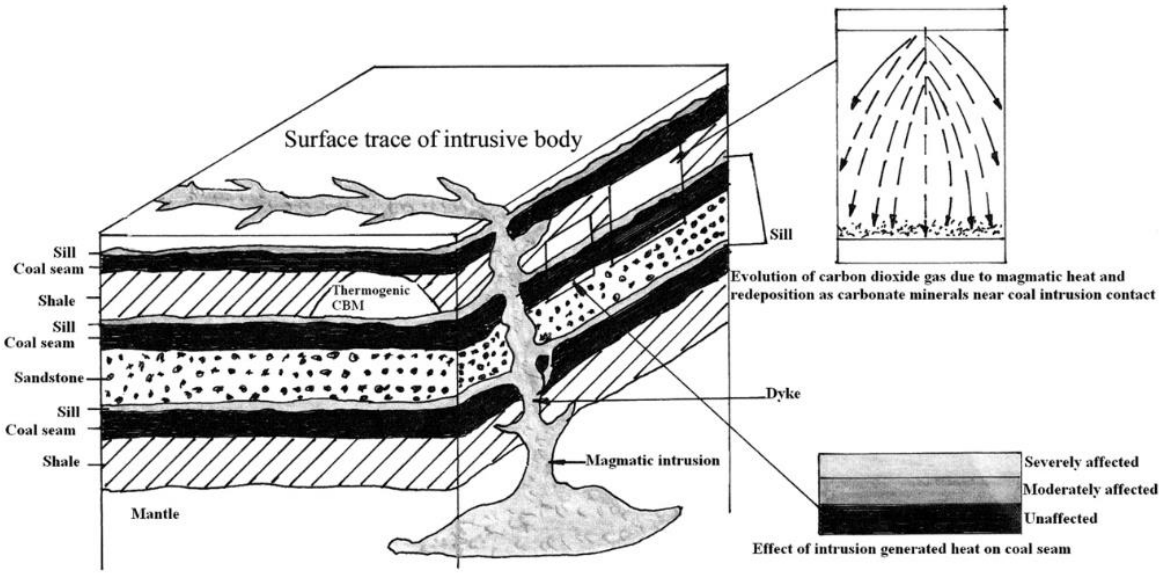

Figure 1. Schematic presentation of magmatic intrusion affecting the coal seam in Jharia Coalfield, Damodar Valley India (Singh, Sharma and Singh, 2008)

Contact with these intrusions causes a relatively local heat flow, resulting in an alteration of the surrounding coal. The overall thermal effect on the coal is dependent on a number of factors, including (Kwiecinska and Peterson, 2004):

- The thickness, nature, form and temperature of the intrusion;
- The duration of the heating;
- The distance from the direct contact; and
- The composition and rank of the intruded coal.

With the composition of the initial coal in mind, it has been observed through laboratory testing that non-coking coals do not form natural coke, but instead form natural char (Singh *et al*, 2007). Natural char is primarily differentiated from natural coke through its lack of mosaic structure (Kwiecinska and Peterson, 2004).

2.2 PROPERTIES OF HEAT-AFFECTED COAL

2.2.1 Physical Properties

The physical properties of coal can be categorised as either macroscopic or microscopic. In terms of macroscopic properties, Kwiecinska and Petersen (2004) state that, in general, heat-affected coal is dull, compact and hard, with pores that are either empty or in filled with mineral matter, especially calcite. Roberts, Warbrooke and Ward (1989) found that, in a heat-affected Newcastle coal, it was dull with numerous white carbonate veins. Closer to the intrusion contact the coal was massive, and then becoming banded with remnants of the original stratification appearing as the distance to the contact increased. Singh *et al* (2007) investigated heat affected coals in the Jharia coalfield, and found micro-cracks and fissures had developed near to the intrusion, as well as pits and cavities of various sizes. The presence of both of these features was attributed to the escape of volatiles in the coal, caused by the intrusion. This generally aligns with the findings of Roberts, Warbrooke and Ward (1989) and Kwiecinska and Petersen (2004). Figure 2 summarises the main macroscopic changes in heat-affected coal.

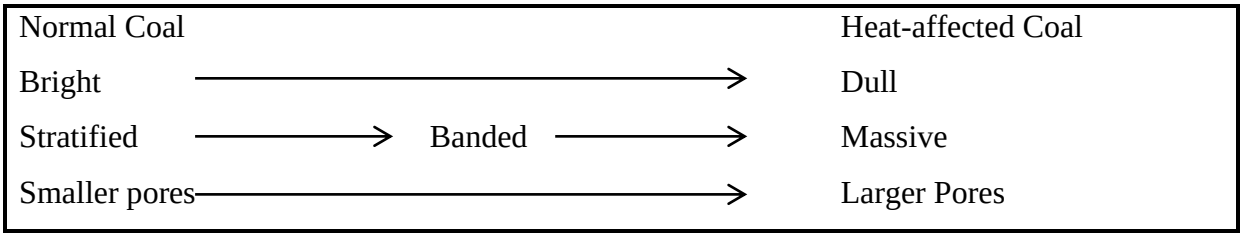

Figure 2. The main macroscopic changes identified in heat-affected coal in comparison to normal coal.

The effect on the microscopic properties is dependent mainly on the initial rank of the coal and its level of maturity at the time of the intrusion. The resulting heat-affected coal can be separated into three groups of microconstituents (Taylor *et al*, 1998):

- The matrix (groundmass) formed by the total alteration of the original coal macerals vitrinite and liptinite;
- The macerals of the inertinite group, which maintain structures and textures visible in the unaltered coal; and
- New components, which are partly high-carbon material and partly mineral matter, formed due to the intrusion.

Kwiecinska and Peteresen (2004) suggest that, at microscopic levels, the heat-affected vitrinite often exhibits a mosaic structure with varying degrees of anisotropy. They also state the reflectance and anisotropy tend to increase with the temperature of the intrusion, reaching a maximum reflectance of up to 11%$R_{o,max}$. Singh, Sharma and Singh (2008) found that, in a sample of heat-affected coal from the Jharia coalfield, the reflectance and anisotropy increased with closer proximity to the intrusion. Roberts, Warbrooke and Ward (1989) also found that, in a heat-affected Newcastle coal, the reflectance increased steadily towards the intrusion, whilst also observing the formation of a mosaic structure.

Kweicinska and Petersen (2004) also give several main microscopic texture types that may be observed in heat-affected coal through the use of scanning electron microscopy, illustrated in Figure 3, including:

- Pores (A);
- Spheres (B);
- Folds (C); and
- Holes (D).

2.2.2 Chemical Properties

The changed composition of heat-affected coals is a defining feature of their chemical properties. The introduction of heat due to the intrusion causes the evacuation of some coal constituents, the introduction of minerals from the intrusion on the intrusion interface, and the metamorphosis of other coal constituents.

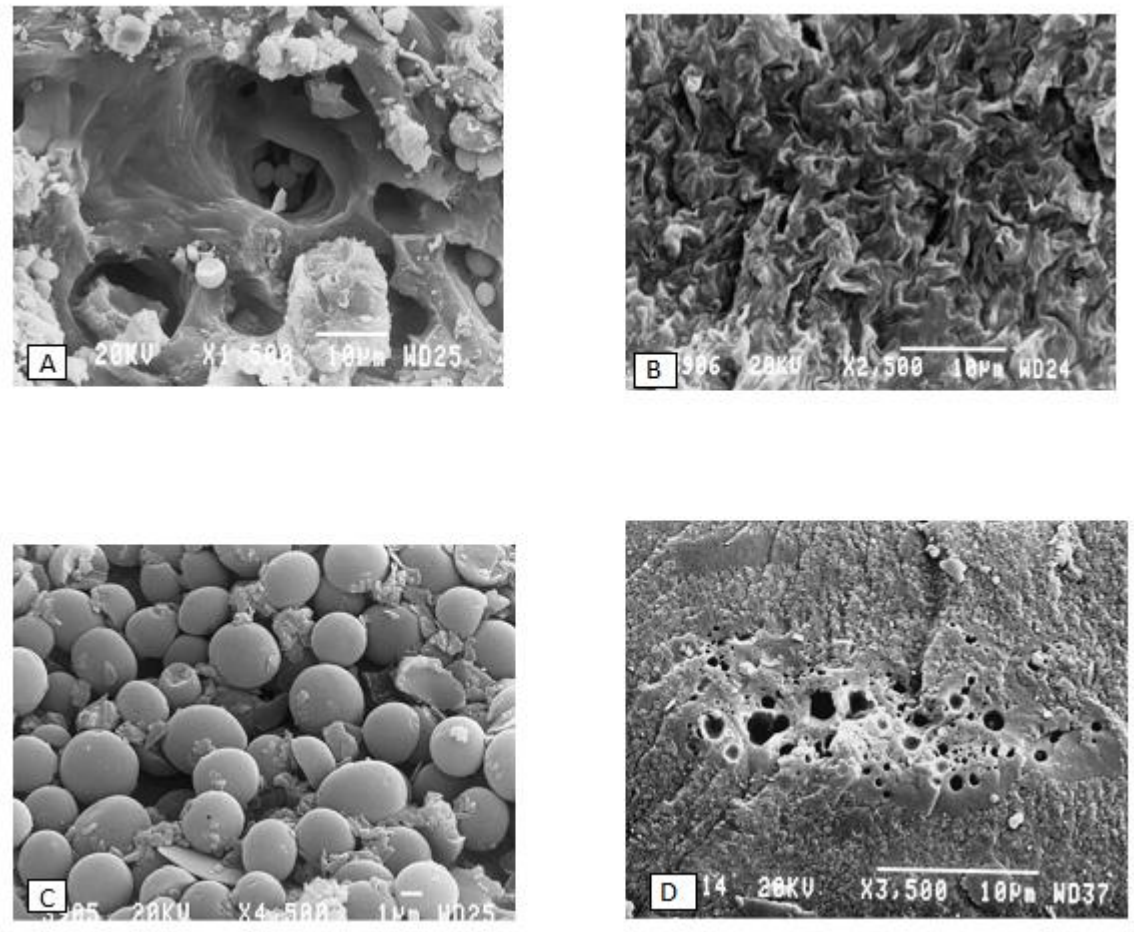

Figure 3. Coal textures observed through scanning electron microscopy (Kweicinska and Petersen, 2004)

A major change is the evacuation of the volatile matter. This has been observed in numerous cases (Yao, Liu and Huang, 2011; Singh, Sharma and Singh 2008; Fredericks, Warbrooke and Wilson, 1985), with the volatile matter content of the coal decreasing nearer to the intrusion. This has the result of artificially increasing the rank of the coal. During this process, chemical cracking of a gaseous phase of the volatile material results in carbonaceous material being deposited. This results in forming a new constituent of coal, as either small spheres, 2-5 μm in diameter, infilling vesicles within thermally altered carbonaceous rocks or as pyrolytic carbon, which can appear in layers, lining or fillings cavities (Kwiecinska and Petersen, 2004). Singh *et al* (2007) observed the presence of pyrolytic carbon in heat-affected Jharia coal. Heat-affected coal has also generally been observed to show an increase in both ash and fixed carbon content, though an increase in ash is not always the case (Rimmer, Yoksoulian and Hower, 2009).

The mineral content of heat-affected coal shows little change, with the main effect being the metamorphosis of pyrite (FeS_2) to either FeS or Fe_2O_3. The crystal shapes of the minerals provide evidence of hydrothermal activity (Singh *et al*, 2007; Kwiecinska and Petersen, 2004).

The main chemical changes that occur in heat-affected coal are summarised in Figure 4.

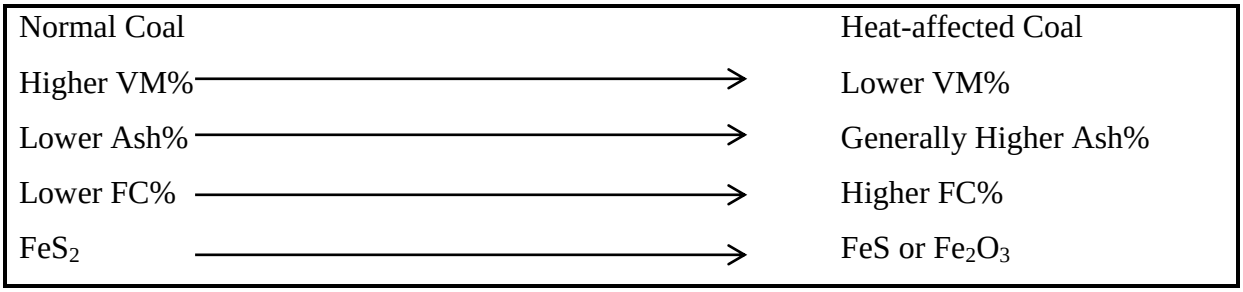

Figure 4. Chemical changes in heat-affected coal compared to normal coal.

3 SELF-HEATING OF COAL

3.1 COAL SELF-HEATING PROCESS

The self-heating of coal is the process by which exothermic oxidation reactions occurring in the coal generate heat. Depending on the conditions of this process, self-heating may generate sufficient heat to reach the ignition point of the coal, resulting in spontaneous combustion.

Self-heating occurs where the presence of oxygen causes oxidation to occur in the coal. During the oxidation process, the positive valence of an element ion is increased, or the negative valence of an element ion is decreased, resulting in a chemical change or breakdown of the compound. Along with the generation of heat, this process also results in the release gaseous emissions, including CO_2, CO and H_2O (Nalbandian, 2010; Qi *et al*, 2016).

Coal oxidation begins as soon as the coal comes into contact with oxygen in the air. This can happen naturally, where the process is known as weathering. Generally, self-heating occurs in coal seams that are exposed to air, coal caved in the goaf of longwall mines, occasional pillar heating in fractured coal, in stockpiled or transported coal, or in coal left in abandoned mines and waste dumps (Wang, Dlugogorski and Kennedy, 2003a).

Wang, Dlugogorski and Kennedy (2003a) state that there are four major phenomena that occur during the oxidation of coal, illustrated in Figure 5, including:

- Oxygen transport to the surfaces of coal particles and within coal pores;
- Chemical interaction between coal and O_2;
- The release of heat; and
- The release of gaseous products.

The chemical reactions and processes that occur during coal oxidation are complicated, owing to the complex and varying composition of coal. Multiple investigations into these processes have been undertaken, and whilst the underlying reactions are not well understood, several models have been proposed.

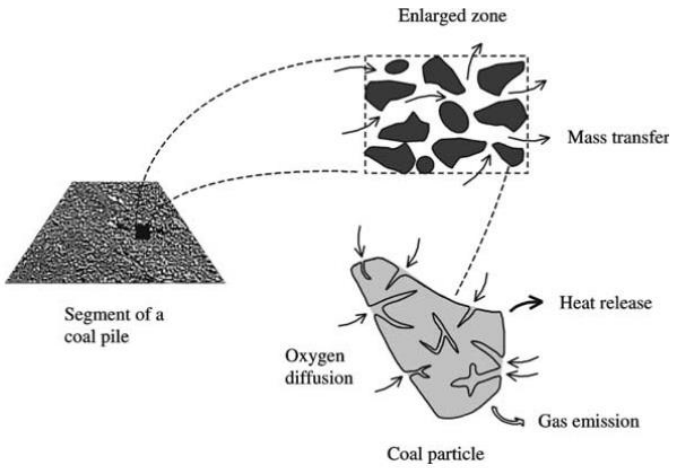

Figure 5. The major phenomena that occur in coal oxidation (Wang, Dlugogorski and Kennedy, 2003a)

Kam, Hixson and Perlmutter (1976) proposed a multiple pathway model in which two parallel reactions occur. Under this model, the first reaction pathway is a direct "burn-off" reaction, which generally resembles combustion. The second pathway involves chemisorption, the formation of oxygenated complexes and the subsequent decomposition of the complexes. These reaction pathways are illustrated in Figure 6.

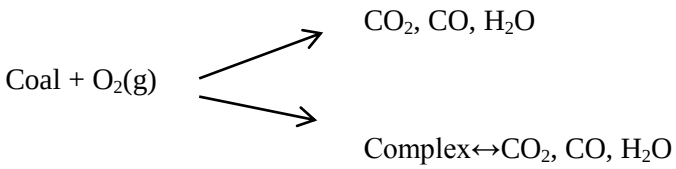

Figure 6. Coal oxidation pathways (Kam, Hixson and Perlmutter, 1976)

Wang, Dlugogorski and Kennedy (2003b) undertook an experimental investigation using an isothermal flow reactor. Using the two parallel reactions model to interpret the data they collected, their results provided supporting evidence for the model. They suggest a similar reaction process to Kam, Hixson and Perlmutter (1976) for the "burn-off" reaction pathway, along with a detailed series of reactions to describe the chemisorption reaction pathway.

Qi *et al* (2016) investigated the reaction pathways involved in coal self-heating using quantum chemistry calculations. Using this method, the authors determined the active sites of functional groups in the chemical structure of coal, and the activation energies of reaction activities. The study selected a typical hydroxyl group containing molecule (Ar-CH_2-

$CH(CH_3)$-OH) as the basis for determining reaction pathways. Figure 7 illustrates their proposed essential reaction mechanism.

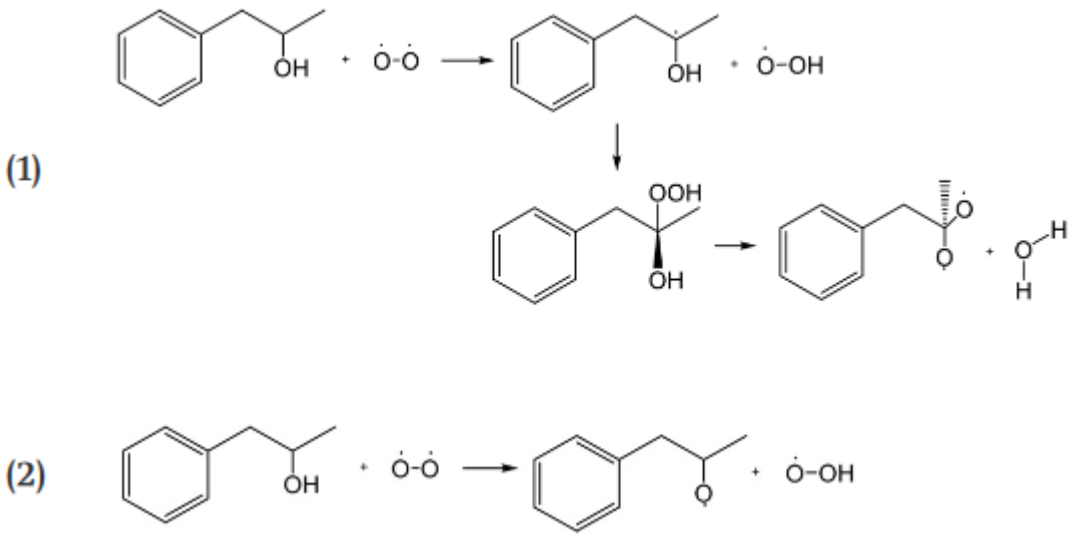

Figure 7. Essential hydroxl reaction mechanism (Qi *et al*, 2016)

3.2 FACTORS AFFECTING COAL SELF-HEATING PROPENSITY

3.2.1 Introduction

There are numerous factors that contribute to the propensity of coal to self-heat. These factors can generally be categorised as either intrinsic, being the fundamental properties of the coal itself; and extrinsic, being the properties of the atmospheric, geological and mining conditions. These factors as identified Kaymakci and Didari (2002) are given in Table 1.

Table 1. Intrinsic and extrinsic factors affecting coal self-heating propensity (Kaymakci and Didari, 2002)

Intrinsic Factors	Extrinsic Factors
Presence of pyrite	Temperature
Moisture	Moisture
Particle size and surface area	Barometric pressure
Coal rank and petrographic constituents	Oxygen concentration
Chemical Constituents	Bacteria
Mineral Matter	Coal seam and surrounding strata
	Method of working
	Ventilation system and airflow rate
	Timbering
	Roadways

3.2.2 Intrinsic Factors

Coal rank is a major indicator of the propensity of coal to self-heat. It is widely recognised that lower ranked coals are more susceptible to spontaneous combustion than higher ranked coals (Kaymakci and Didari, 2002).

Coal rank is the measure used to indicate the stage of coalification that a coal has reached. Coalification is the process whereby vegetation is transformed through heat and pressure into coal. Initially peat is formed, which is then transformed to lignite, then to sub-bituminous coal, then to bituminous coal, and finally to anthracite. This process is illustrated in Figure 8

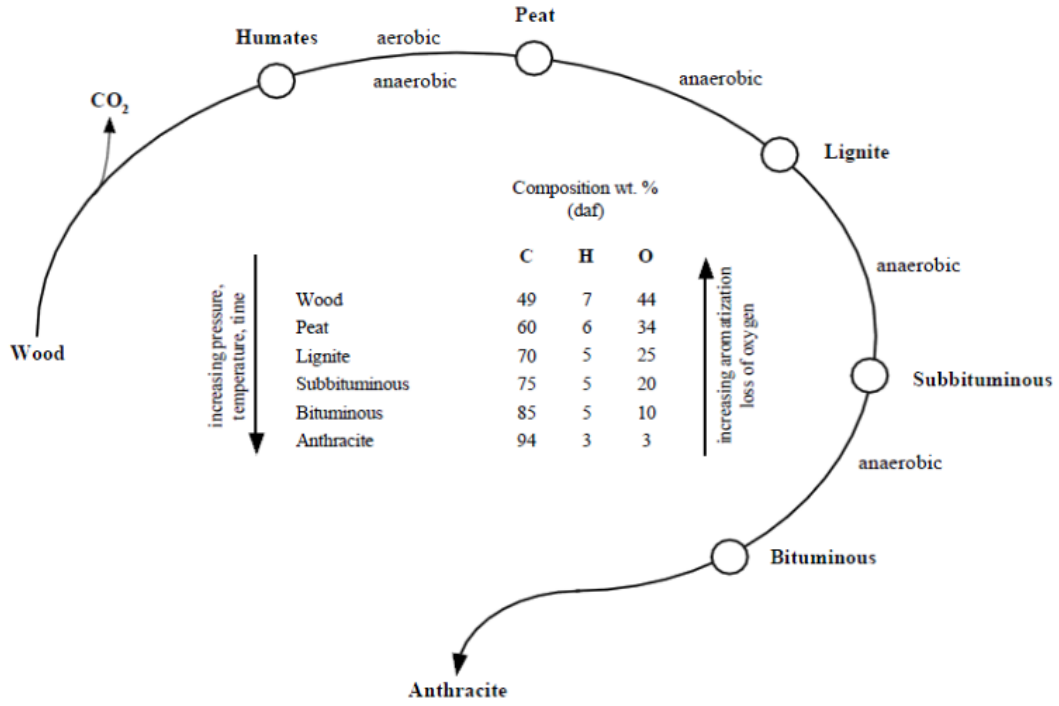

Figure 8. Schematic representation of the coalification process (Wang, 2014).

Beamish (2005) undertook a study in order to link the propensity of a coal to self-heat to its Suggate rank. The Suggate rank was developed and updated by Suggate (2000) in order to provide a quantitative ranking system for New Zealand and Australian coals. This system is demonstrated in Figure 9, giving Suggate rankings based on a coals calorific value and volatile matter content on a dry mineral matter and sulphur free basis. Under this system, coals of a higher Suggate ranking have undergone a greater degree of coalification.

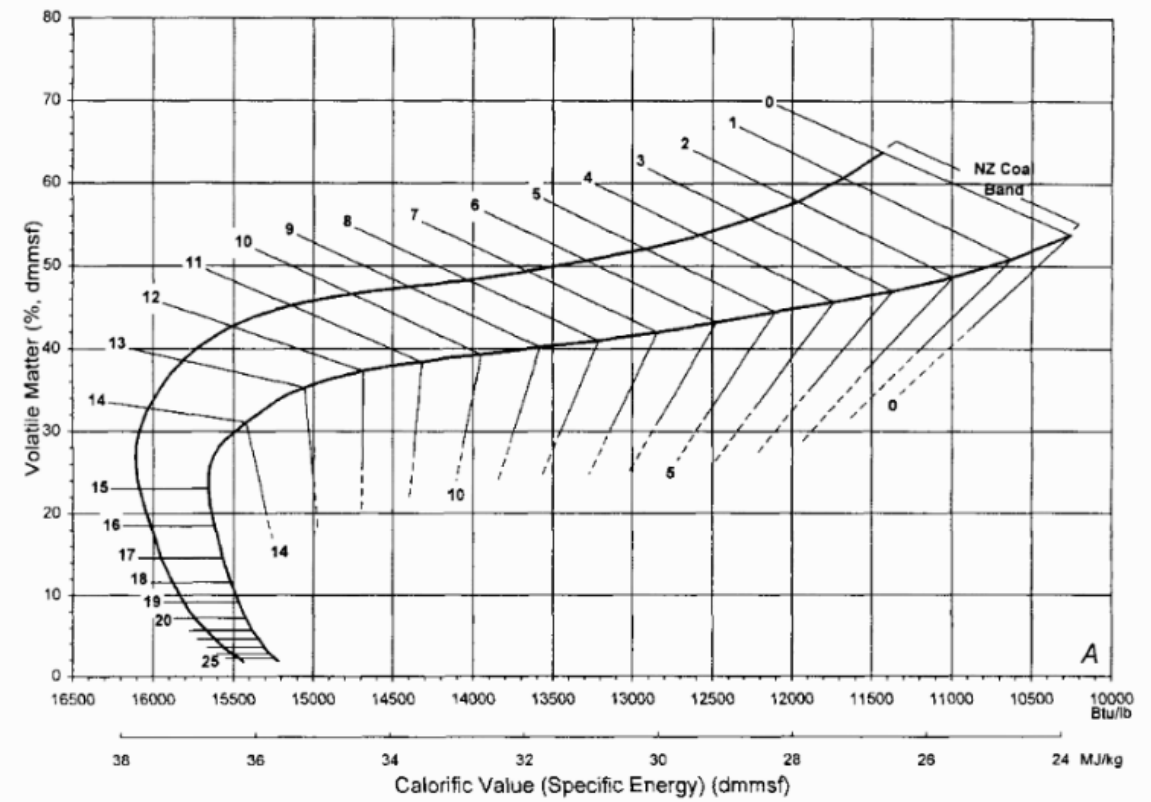

Figure 9. The Suggate ranking scale (Suggate, 2000)

Beamish (2005) found that the self-heating propensity of coals follows a well-defined relationship in accordance with their rank. Arisoy and Beamish (2008) more recently found a similar relationship, illustrated in Figure 10. This relationship demonstrates the increasing propensity for self-heating with the increasing rank of coal. While the relationship in Figure 10 might imply that sub-bituminous coals are approximately 20 times more susceptible to self-heating compared to high volatile bituminous coals, once coal quality parameters including moisture and mineral matter content are taken into account, this difference may be reduced to approximately 2 to 3 times.

The chemical constituents of coal also have an impact on a coals propensity to self-heat. Moisture, ash and pyrite content all have distinctive effects. Kaymakci and Didari (2002) state that pyrite content may increase self-heating propensity, changes in moisture content can have apparent effects, and ash content generally decreases the self-heating propensity.

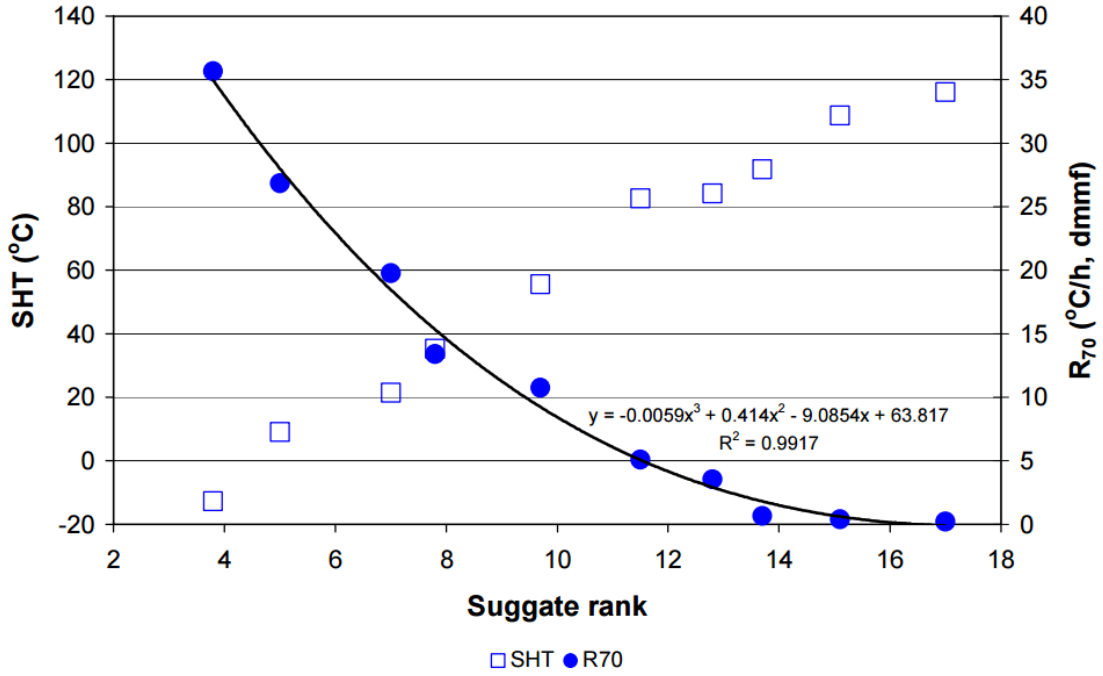

Figure 10. Relationship beween coal rank and spontaneous combustion index parameters SHT and R70 (Arisoy and Beamish, 2008).

Ash is formed from most of the mineral matter when coal is burned. Beamish and Blazak (2005) conducted a study on Callide coals, and found that the propensity for a coal to self-heat negatively correlates to its ash content. This relationship is illustrated in Figure 11. The proposed mechanism of this effect is the mineral matter in the coal acting as a heat sink.

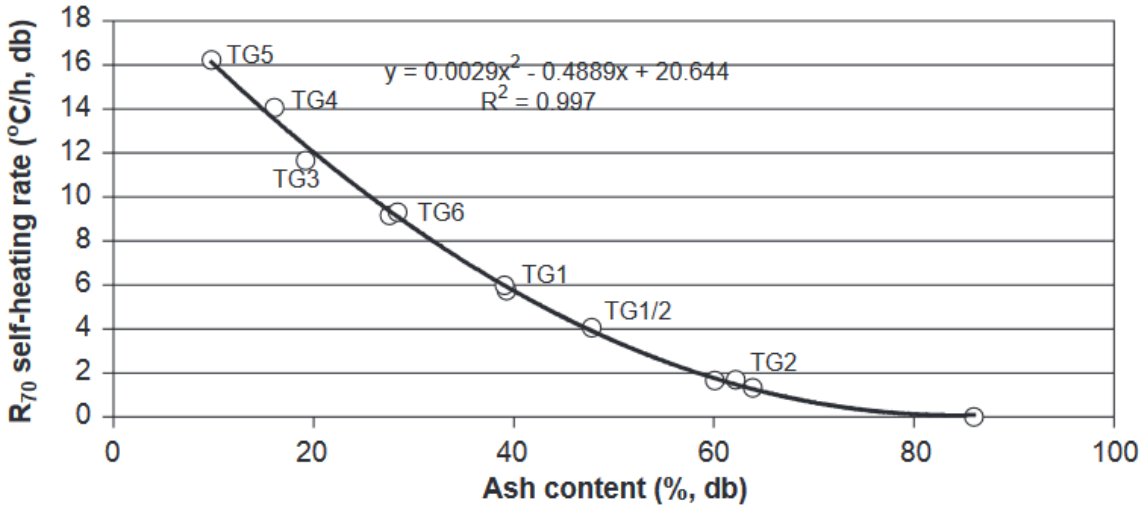

Figure 11. Relationship between ash content and R70 self-heating rate of Trap Gully coal (Beamish and Blazak, 2005)

The moisture content of coal has a complex effect on its propensity to self-heat. Because of waters high specific heat, and through evaporation, water can absorb large amounts of heat from the coal, making it difficult for heat to accumulate in the coal. Moisture can also obstruct oxygen form accessing the surface of the coal, inhibiting self-heating due to oxidation (Xu, Wang and He, 2013).

Beamish and Hamilton (2005) found that, as the moisture content of coal was progressively increased, its propensity for self-heating decreased dramatically. This relationship is demonstrated in Figure 12.

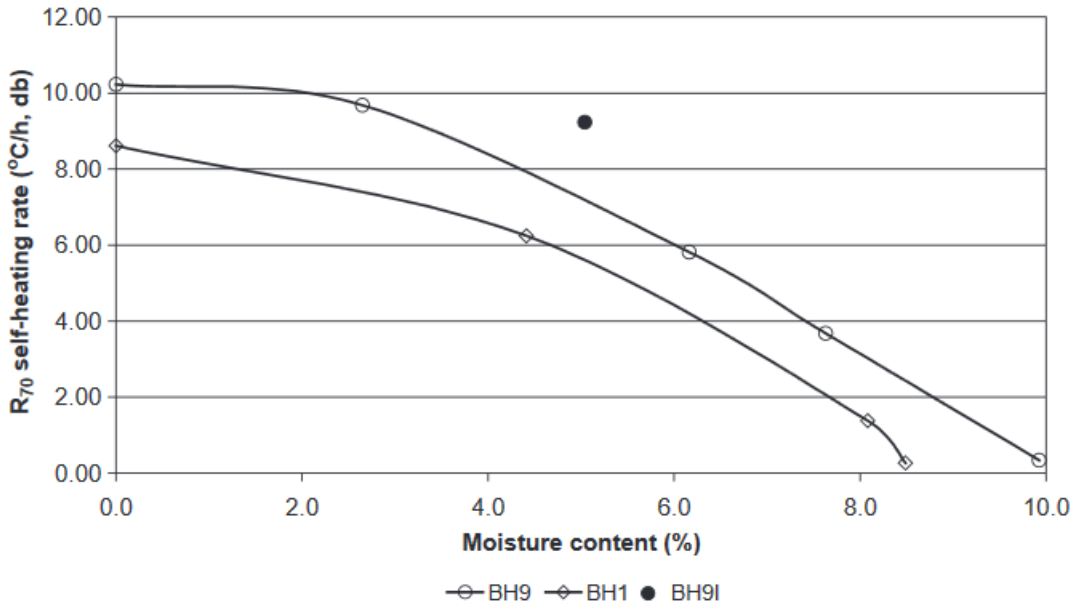

Figure 12. Relationship between moisture content and R70 self-heating rate of Boundary Hill coal (Beamish and Hamilton, 2005)

The pyrite content of coal also influences its propensity to self-heat. At concentrations of above 2%, pyrite is generally considered a self-heating accelerant. This, however, also depends on the type of pyrite present and not simply the amount of pyrite. Pyrite also requires the presence of moisture to react effectively, without which it does not contribute to the self-heating process (Arisoy and Beamish, 2015).

Deng *et al* (2015) found that coal with a pyrite content of 5% promoted self-heating the most in terms CO of production, whereas coal with a pyrite content of 7% promoted self-heating the most in terms of heat flux.

The porous nature of coal is another property that influences its propensity to self-heat. In general, a greater pore volume will allow for a higher amount of oxygen to come into contact with the coal, in turn leading to more oxidation occurring and hence increasing a coals propensity to self-heat (Dudzinska, 2014). Dudzinska was able, through experimental study, to link the increase of both micropore volumes and macropore surface area with an increase in the propensity to self-heat. Micropore volume was found to be a more useful indicator than macropore surface area, however.

Finally, the particle size of coal also has an effect on self-heating propensity. A smaller particle size will give a greater surface area, allowing a larger interface for oxygen to react with the coal, generating heat. Particle sizes smaller than a critical value, however, have little effect on self-heating (Kucuk *et al*, 2003).

3.2.3 Extrinsic Factors

Ambient temperature is an important factor for coal self-heating in terms of its potential to reach thermal runaway, resulting in spontaneous combustion. For a given coal, there is a critical ambient temperature for thermal runaway to take place (Yuan and Smith, 2012). Therefore, the starting temperature of the coal is an important factor in whether this critical ambient temperature is reached. Arisoy and Beamish (2015) found that coal oxidation sites are reduced to a limiting value as oxidation takes place. Consequently, the formation of oxidation reaction products decreased with the extent of oxidation. The starting temperature of the coal correlates to both the limit value reached, with a higher limit value for higher temperatures; as well as the time taken to reach this value. As such, it is possible for some coals with a low enough starting temperature to never reach the critical ambient temperature.

Ventilation is a complex factor in coal self-heating, as an air supply will provide oxygen whilst carrying away heat from the coal. There is a critical air quantity that will allow the coal to oxidise whilst not removing enough heat to stop it from accumulating, favouring the overall heating of the coal (Kaymakci and Didari, 2002). Yuan and Smith (2012) found that, with a sufficient volume of ventilation, coal could reach thermal runaway from a lower critical temperature compared with unventilated coal. However, they also indicated that ventilated coal may take a much longer time to reach ignition compared with unventilated coal.

The moisture content of the air is also a factor in coal self-heating. Dry air flowing over a relatively moist coal will remove moisture from the coal and cause a temperature decrease. Moist air flowing over a relatively dry coal will add water to the coal through adsorption, resulting in a temperature increase. However, in normal circumstances coal always contains some moisture, being in near equilibrium with the surrounding air, meaning that heating will generally be only caused by oxidation (Kucuk *et al*, 2003).

3.3 MEASURING COAL SELF-HEATING

3.3.1 Differential Scanning Calorimetric (DSC) Technique

The DSC technique has been used to assess the propensity for self-heating in coal. The technique involves measuring the difference in energy inputs into a substance (in this case coal) and a reference material under a controlled temperature program. Thermal events in the sample appear as deviations from the reference material baseline, with endothermic events usually represented as being negative (below the baseline). This corresponds to an increased transfer of heat to the coal sample relative to the reference material.

The experimental set up required to undertake DSC testing comprises the differential scanning calorimeter, sample holder, crucible sealing press (crimper), purge gas supply arrangement, a computer and a graph plotter. The parameters used in testing are not standardised, and a variety have been used. Therefore the results of differing tests have not allowed for the creation of a standardised index for self-heating propensity (Mohalik *et al*, 2009).

3.3.2 Differential Thermal Analysis (DTA) and Thermal Gravity (TG)

Coal self-heating propensity has been examined through the use of DTA and TG. Heat generation and weight changes during the analysis produce DTA and TG curves, which have been used for both general propensity and kinetic analysis (Zhang, Gao and Zhang, 2015).

3.3.3 Crossing-Point Temperature (CPT) Method

The CPT method is widely used to assess the propensity of coal to self-heat. This method involves placing samples of coal into a reaction vessel, which is then placed in a programmed temperature enclosure. Dry air with a known oxygen concentration is preheated in the temperature enclosure to match its temperature before being directed into the reaction vessel. The temperature in the oven is then increased at a constant rate, which in turn increases the temperature of the air flow to the reaction vessel. Both the temperature of the temperature enclosure and the reaction vessel are logged. The crossing-point temperature of the coal is

when the temperature in the reaction vessel matches the temperature in the temperature enclosure. A schematic of the system is given in Figure 13 (Xuyao *et al*, 2011).

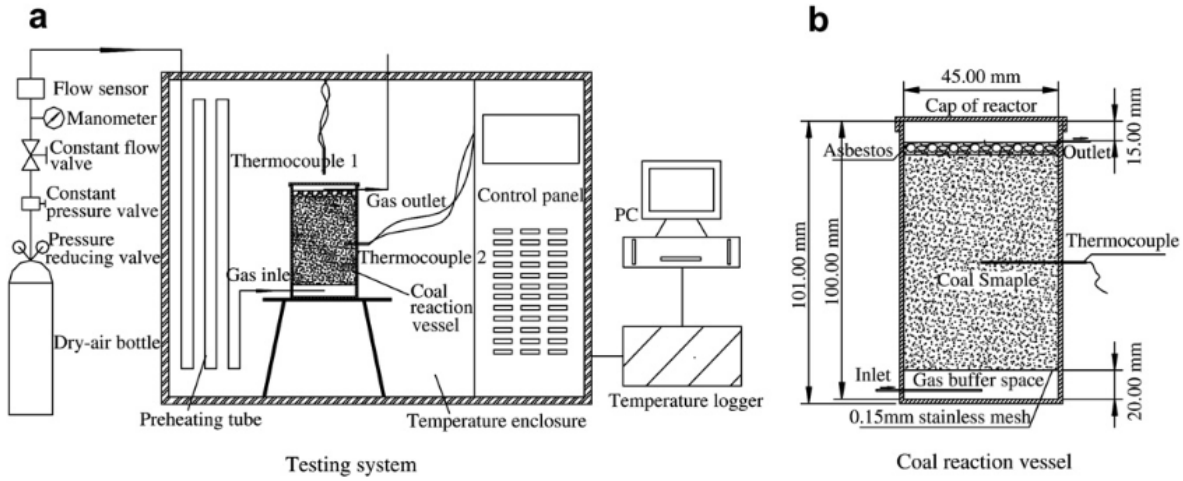

Figure 13. Schematic of crossing-point temperature testing system (Xuyao *et al*, 2011)

3.3.4 Wet Oxidation Potential (WOP) Method

The WOP method is a recent electro-chemical method for determining the propensity of coal to self-heat. The method involves using a beaker containing potassium permanganate in potassium hydroxide solution, with a calomel reference electrode and carbon electrode immersed in it. When the potential difference, measured using a millivoltmeter, reaches a stable reading, a sample of coal is added to the mixture, which is then continuously stirred using a magnetic stirrer. The potential difference and temperature of the mixture are recorded until the potential difference reaches a stable value. The experimental set-up is demonstrated in Figure 14 (Ray and Panigrahi, 2015).

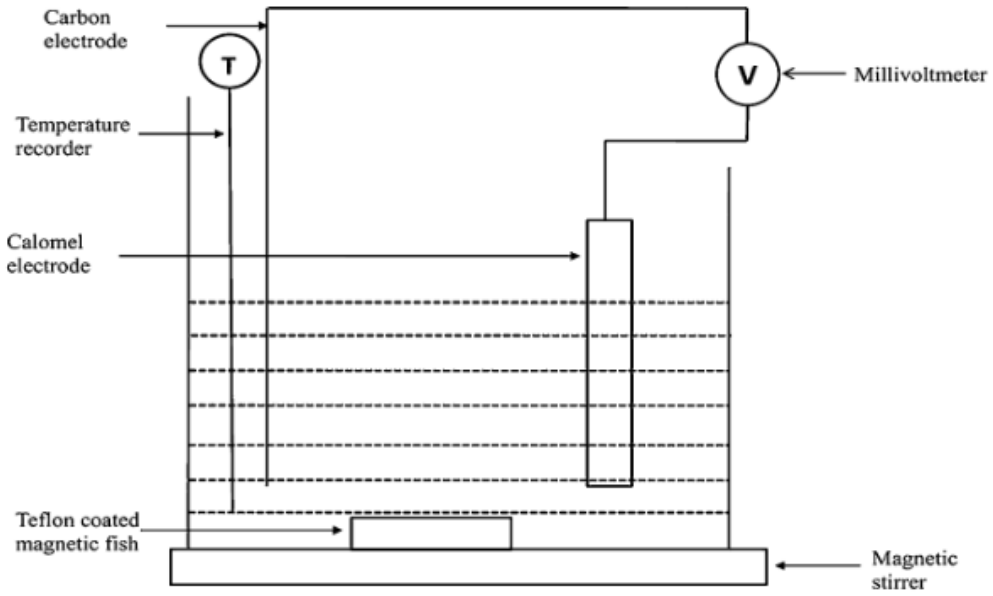

Figure 14. Schematic of experimental set-up for WOP method (Ray and Panigrahi, 2015).

3.3.5 The R_{70} Testing Method

The R_{70} test is commonly used to provide an index rating for the propensity of a coal to self-heat. The testing procedure involves drying a 150 g sample of <212 mm crushed coal at 110°C under nitrogen for approximately 16 hours. Whilst still under nitrogen, the coal is cooled to 40°C, and then transferred to an adiabatic oven. Once the coal has stabilised at 40 °C, oxygen is passed through the sample at 50 mL/min, and the temperature rise due to self-heating of the coal is recorded from 40 °C to 70 °C. The average rate of temperature rise between these values is the self-heating rate index (R_{70}), given in units of °C/h. This index indicates the self-heating propensity of the coal sample (Beamish, Hogarth and Jabouri, 2005). A schematic diagram of the reaction vessel is included in Figure 15.

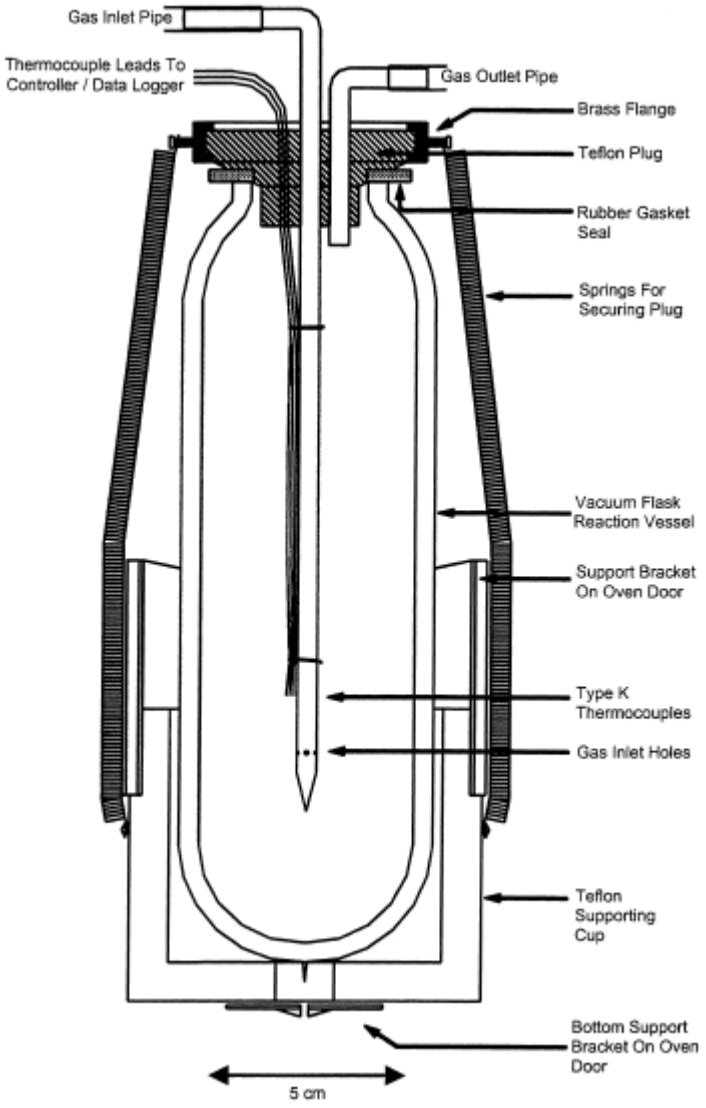

Figure 15. Schematic diagram of R_{70} reaction vessel (Beamish, Barakat and St George, 2000)

The widespread use and standardisation of this method mean that results obtained can be meaningfully compared to the results given by other researchers. This is, therefore, a very suitable method to use for the testing undertaken in this project.

3.4 COAL SELF-HEATING KINETICS

The kinetics of the coal oxidation reaction is another important aspect to be considered when investigating the self-heating of coal. Kinetics deals with the rate of reaction, and in this case, the rate of the oxidation reaction of coal. Understanding this process is important in order to accurately model and predict self-heating behaviour. The kinetic behaviour of the coal oxidation process has normally been modelled using the conventional Arrhenius equation, given in Equation 1 (Arisoy and Beamish, 2015).

$$\frac{d\rho_{ox}}{dt} = \rho_{ox}^{0} \cdot Aexp\left(\frac{-E}{RT}\right) \quad (1)$$

Jones and Newman (2003) investigated the kinetics of coal oxidation using microcalorimeter analysis, and found that non-Arrhenius behaviour was displayed by some coals. Further investigation by Arisoy and Beamish (2015) indicated, through adiabatic testing, that the coal oxidation reaction displays non-Arrhenius behaviour at low temperatures, converging to Arrhenius behaviour at higher temperatures. Figure 16 illustrates this behaviour, from various starting temperatures, through an Arrhenius plot.

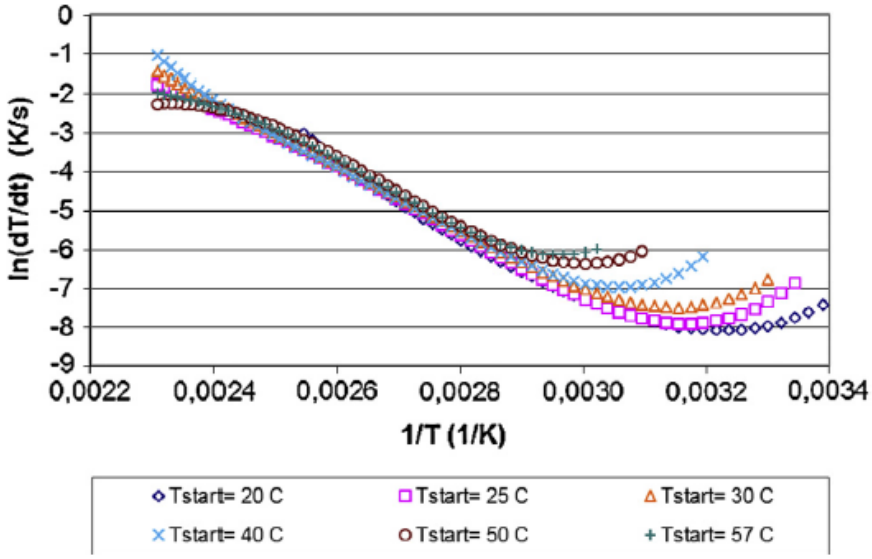

Figure 16. Reaction rate curves fitted to the measured data from repeat testing of a Hunter Valley high volatile bituminous coal at different starting temperatures (Arisoy and Beamish, 2015).

This behaviour has important implications for understanding the self-heating of coal, particularly in the time it takes for thermal runaway to be reached, and warrants further investigation.

3.5 Spontaneous Combustion and Risk Management

Spontaneous combustion through the self-heating of coal is the most significant cause of fires in coal mines throughout the world, and a major cause of coal fires in related industries (Stracher, 2007). Spontaneous combustion can be the final result of coal self-heating if the heating is sufficient for ignition to take place.

Because of the complexity of the coal self-heating process, it is difficult to predict spontaneous combustion events. Therefore, mine operators often rely on detection methods in order to assess its occurrence. These methods include temperature or heat measurements, index gases, numerical modelling and the radon method, with index gases being the most commonly used (Xie *et al*, 2011).

The outcomes of a spontaneous combustion event, if not managed, have the potential to be severe. Many lives have been lost as a result of coal fires caused by spontaneous combustion. Aside from the immediate danger to workers, the economic costs associated with managing the fire, along with the loss of potential product and time are significant impacts. Further, the more common environmental and social impacts caused by coal fires are (Stracher, 2010):

- Visual impacts and the loss of potentially valuable acreage;
- Destruction of the nearby ecosystem;
- Forest fires;
- Windblown dust and siltation of streams;
- Destruction of personal and public property;
- Disruption of families and communities;
- Physical hazards from collapse or explosion;
- Health hazards due to respiration of dust and aerosols, exposure to acidic gases, potentially toxic trace elements and organic compounds;
- Pollution of surface and ground water;
- Loss of valuable energy resources; and
- Significant emission of the major greenhouse gas carbon dioxide (CO_2).

In order to manage the risk of spontaneous combustion, the development of PMHMP is integral. A skeleton for the development of a spontaneous combustion management plan is as follows (Cliff, Brady and Watkinson, 2014):

1. Introduction – including overview, scope and policy
2. Consultation
3. Risk Identification
4. Risk analysis and evaluation
5. Risk management controls

6. Monitoring – including inspections, gas monitoring and Trigger Action Response Plans (TARPS)
7. Information –documents that support the plan
8. Training
9. Roles and responsibilities
10. Supervisors
11. Audit
12. Review
13. References
14. Appendices

The management of spontaneous combustion risk involves both proactive and reactive controls. For underground mines the most important proactive control in the appropriate design of mining operations, through the use of computational simulation. Control over pressure differentials around goafs and use of inertisation are also utilised in order to reduce the potential for oxidation to occur in sealed areas. Reactive controls include the use of monitoring to detect the development of spontaneous combustion, inertisation, ventilation control, and fillers and sealants to react to and manage incidents (Cliff, Brady and Watkinson, 2014).

For open cut mines, the management of spontaneous combustion applies to *in-situ* coal, as well as spoil and stockpiles. Guiding principles for spoil and stockpile management as identified by Carras *et al* (2005) includes:

- Identify and control all fuel sources going to spoil;
- Minimise quantity of fuel going to spoil;
- Reduce oxygen pathways in spoil and stock piles; and
- Avoid dumping hot materials.

Methods for preventing self-heating in spoil piles include the controlled placement of carbonaceous overburden and partings within inert pockets, covering all final surfaces with a layer of inert material, compacting intermediate and final surfaces, clay capping and measures to reduce erosion (Carras *et al*, 2005).

4 HEAT-AFFECTED COAL AND SELF-HEATING PROPENSITY

4.1 ESTABLISHED FINDINGS

Beamish, Cosgrove and Theiler (2016) undertook an investigation into the self-heating behaviour of heat-affected coal. Coal samples from the Mandalong Mine were tested using an adiabatic oven. They found that, whilst the heat-affected coal showed an initial rise above ambient temperature due to self-heating, it was not capable of maintaining this. The normal coal, however, displayed self-heating sufficient to reach thermal runaway. This behaviour is illustrated in Figure 17.

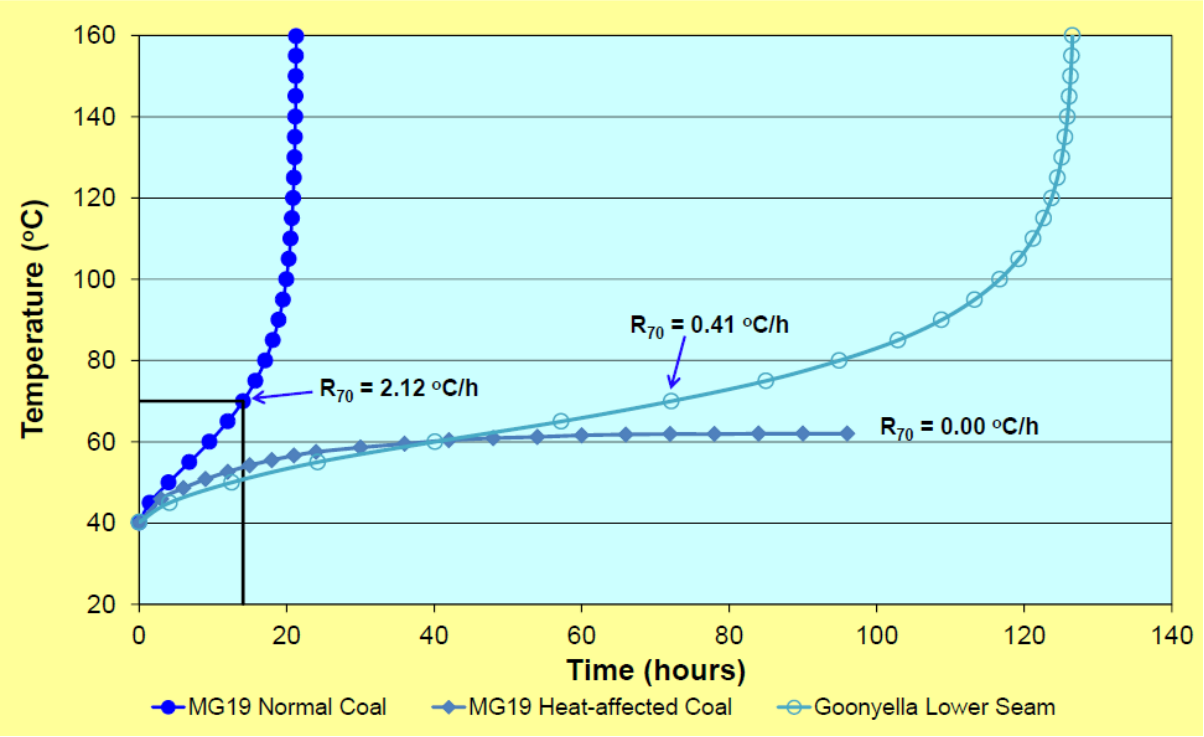

Figure 17. Adiabatic R70 self-heating curves for normal and heat-affected coal from MG19, Mandalong Mine compared against high rank bituminous coal from the Goonyella Lower Seam (Beamish, Cosgrove and Theiler, 2016).

The initial heating in the heat-affected coal was attributed to its vesicular nature, allowing for easy access to open pores for oxidation to take place. However, the thermal alteration of the coal contributes to the destruction of reactive sites and makes access to the remaining sites in the micropore system of the coal more difficult, resulting in the later reduced self-heating effect.

5 EXPERIMENTAL METHOD AND RESULTS

5.1 EXPERIMENTAL METHOD

In order to determine the propensity of selected coal samples to self-heat, the standard R70 testing procedure was used. The testing procedure involves drying a 150 g sample of <212 mm crushed coal at 110°C under nitrogen for approximately 16 hours. Whilst still under nitrogen, the coal is cooled to 40°C, and then transferred to an adiabatic oven. Once the coal has stabilised at 40 °C, oxygen is passed through the sample at 50 mL/min, and the temperature rise due to self-heating of the coal is recorded from 40 °C to 70 °C. The average rate of temperature rise between these values is the self-heating rate index (R_{70}), given in units of °C/h. This index indicates the self-heating propensity of the coal sample. Furthermore, individual data points were recorded throughout the procedure in order to enable a kinetic analysis to be undertaken.

Samples have been taken from various coals, including:

- A range of four heat-affected samples taken from a US mine site;
- A normal sample taken from the same US site; and
- A range of four normal samples taken from various Australian mine sites.

The heat-affected samples were selected at various distances from an igneous intrusion at the site. The normal Australian coals were specifically selected due to their ranks, in order to provide a comparison with the similarly ranked heat-affected coals.

.

In order to determine the rank of each coal, and investigate the effects of the chemical composition, a proximate analysis has also been undertaken for each sample.

5.2 RESULTS

The proximate analysis data is summarised in Table 2. The full data obtained is provided in Appendix A. The heat-affected samples are ordered based on their distance from the igneous intrusion, with 6R being the closest and 5R being the furthest, and are indicated by (h), and the Australian samples are marked RB.

Table 2. Summary of Proximate Analysis Results

Sample ID	Ash Content (%)	Volatile Matter (%)	Fixed Carbon (%)	Volatile Matter (dmmsf)	Calorific Value (dmmsf)
5R (h)	2.9	30.4	65.1	31.1	15524
7R (h)	4.8	24.8	68.9	25.5	15559
8R (h)	6.6	24.1	67.8	25.0	15658
6R (h)	9.3	20.0	69.2	20.6	15777
3R	1.6	39.0	55.5	40.8	14681
8RB	16.6	30.4	51.0	35.5	15344
3RB	4.9	28.8	64.7	30.2	15555
4RB	12.7	18.0	68.5	19.3	15636
1SB	4.5	36.6	57.2	38.3	15359

The volatile matter of the heat-affected coals is lower as the coal is closer to the igneous intrusion, and is significantly reduced in all samples when compared to the normal coal from the same site. This serves to confirm the heat-affected nature of these samples, as a reduced volatile matter content due to the evacuation of the volatiles is a significant feature of heat-affected coal.

Based on the proximate data, the Suggate Rank was determined for each sample, and is presented in Figure 18.

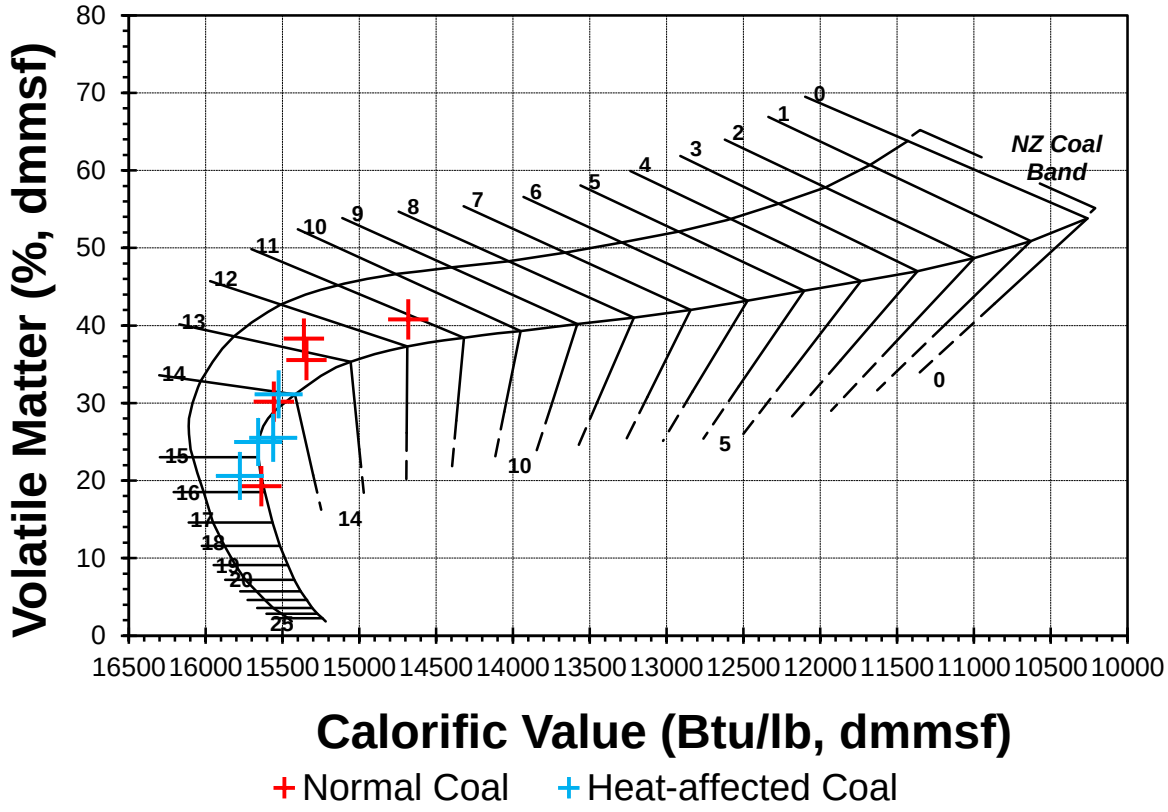

Figure 18. Suggate Rank of tested samples.

The raw data collected for each sample has been included in Appendix B. A graphical representation of this data is given in Figures 19 and 20.

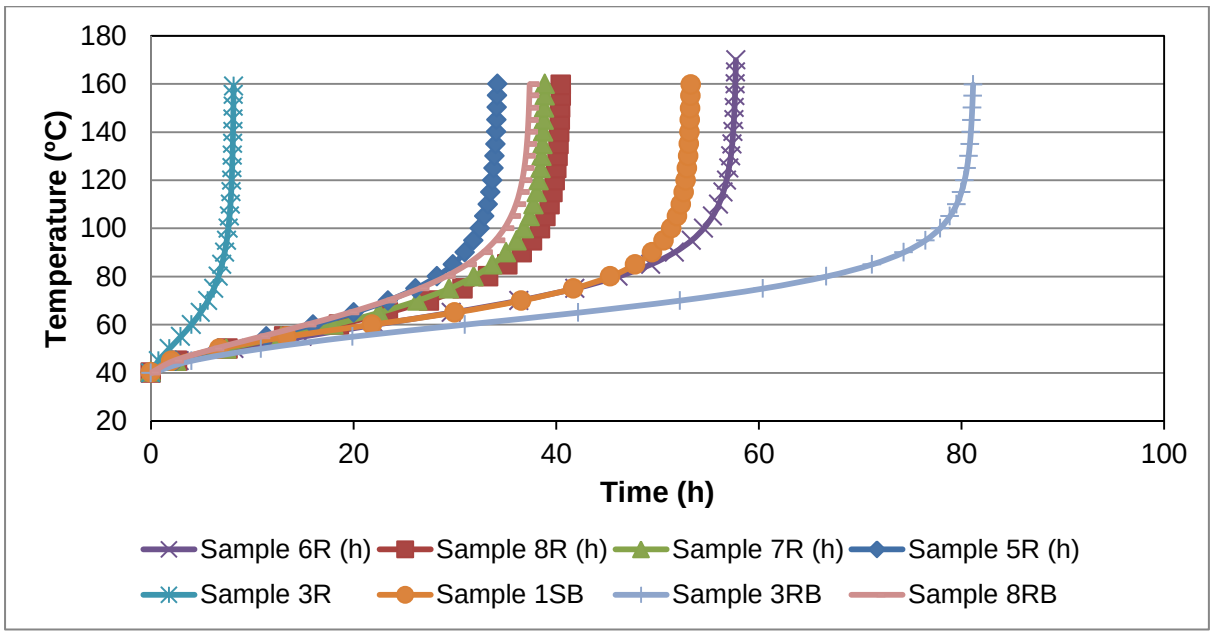

Figure 19. Temperature of samples over time during adiabatic testing (exluding sample 4RB).

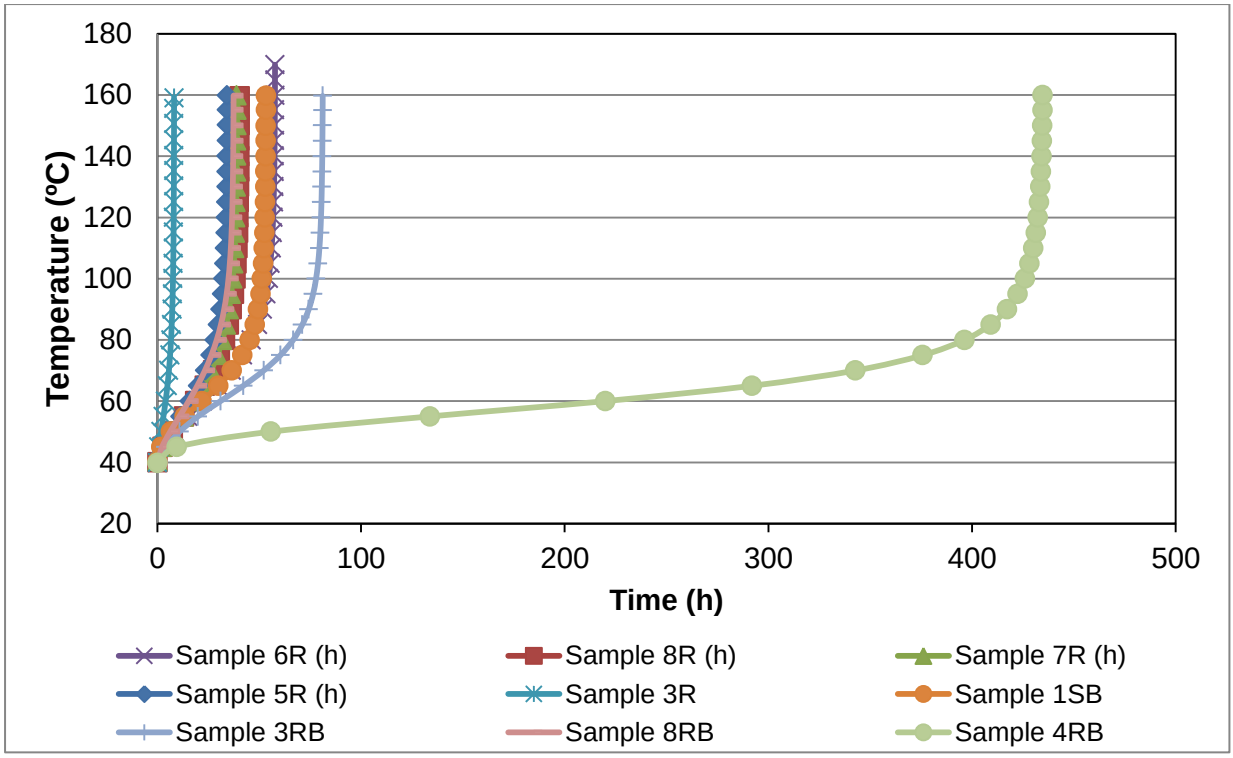

Figure 20. Temperature of samples during adiabatic testing over time (including sample 4RB)

6 ANALYSIS OF SELF-HEATING RESULTS

6.1 R70 DATA ANALYSIS

A summary of the R70 values generated for each sample is given in table x.

Table 3. R70 values for tested samples.

Sample ID	R70 Value (ºC/h)
5R	1.27
7R	1.12
8R	1.09
6R	0.83
3R	5.35
8RB	1.29
3RB	0.58
4RB	0.09
1SB	0.82

These results indicate there is a link between the thermal metamorphosis of coal due to igneous intrusion and its propensity to self-heat. The heat-affected samples exhibit a much lower propensity to self-heat when compared to the normal sample from the same site. Furthermore, as the heat-affected samples are presented in decreasing order of distance to the intrusion, there is a clear trend between the coals propensity to self-heat and the degree to which it has been heat-affected. From this data alone it might seem that heat-affected coal is less prone to self-heating than normal coal. However, examining the remaining normal samples indicates that the relationship is more complicated.

In order to better understand this relationship, its underlying causes were investigated. Given that the process in forming heat-affected coal generally artificially increases its rank, in conjunction with the fact that higher ranked coals generally have a lower propensity to self-heat, the effect of this rank increase was investigated. The Suggate Rank of each sample was plotted against its R70 value, presented in Figure 21.

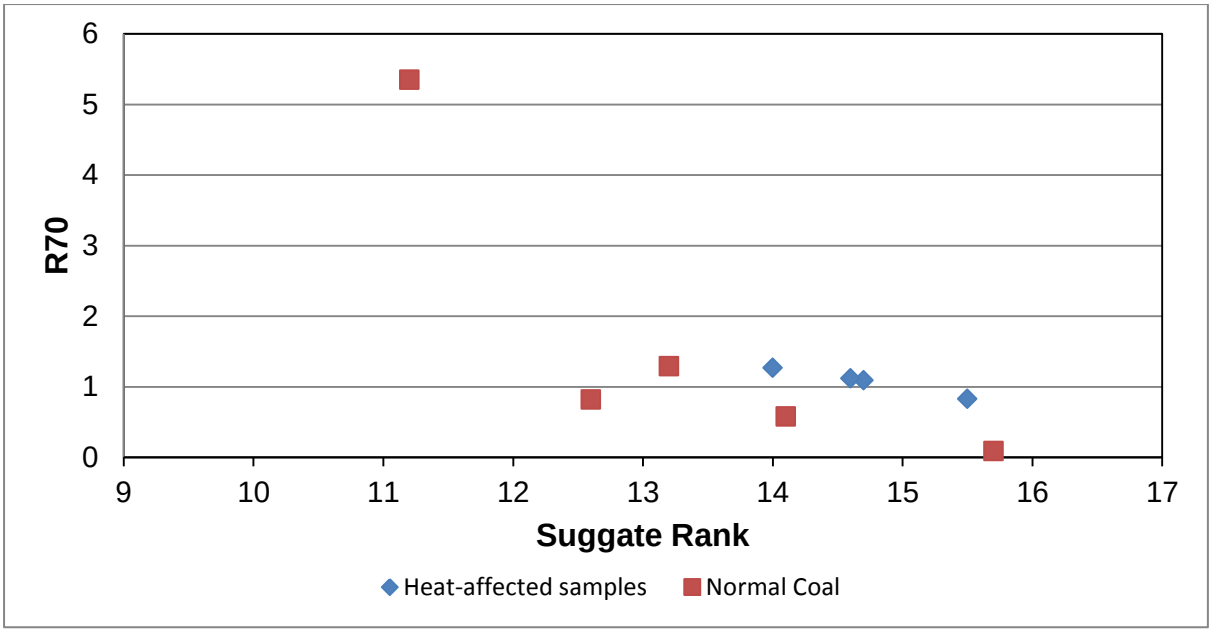

Figure 21. Plot of R70 value against Suggate rank for heat-affected and normal samples.

Evident in the normal coal samples is the non-linear relationship between the rank and the self-heating propensity. The heat-affected samples, however, tend to fall above this relationship, suggesting that they have a higher propensity to self-heat than normal coal of a similar rank.

In order to investigate the causes of this phenomenon, two pairs of samples of similar rank were compared, with one normal and one heat-affected sample in each pair. The chemical composition of each pair was first examined, and is presented in Tables 4 and 5.

Table 4. Chemical composition of samples 6R and 4RB.

Sample ID	R70	Suggate Rank	Ash Content	Volatile Matter Content	Sulphur Content
6R (h)	0.83	15.5	9.3	20.0	1.11
4RB	0.09	15.7	12.7	18.0	0.37

Table 5. Chemical Composition of samples 5R and 3RB

Sample ID	R70	Suggate Rank	Ash Content	Volatile Matter Content	Sulphur Content
5R (h)	1.27	14	2.9	30.4	0.71
3RB	0.58	14.1	4.9	28.8	0.35

In both cases, the heat-affected coals have lower ash contents and higher sulphur contents compared to the normal coals. These discrepancies, however, are minor and are unlikely to be the cause of the significant differences in self-heating susceptibility of the coals.

Having investigated the chemical differences between the heat-affected and normal coal, the physical differences were examined. The key to the different physical properties of heat-affected coal lies in its formation through artificial rank advancement. Whilst a normal coal is naturally rank advanced as a result of both heightened pressure and temperature, a coal that undergoes artificial rank advancement experiences only heightened temperature. This dissimilarity results in the varying physical structure displayed by each coal on a microscopic level, as illustrated in Figures 22 and 23.

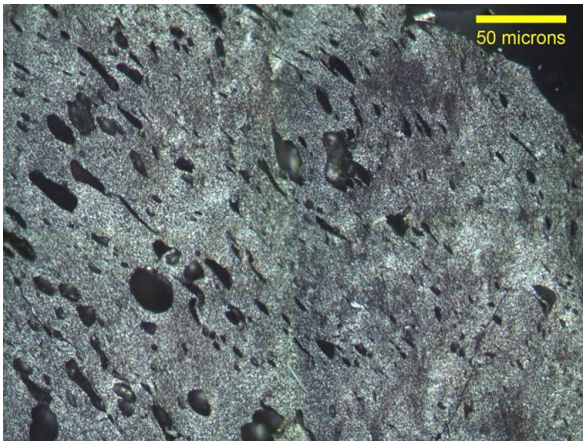

Figure 22. Microscopic structure of heat-affected coal displaying mosaic structure (Beamish, 2016)

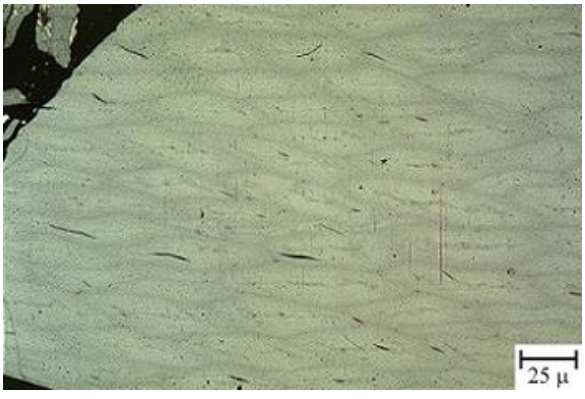

Figure 23. Microscopic structure of naturally rank advanced coal (Southern Illinois University, 2016)

The lack of pressure experienced by the heat-affected coal allows the formation of a mosaic structure with large, open pores which can be clearly seen in Figure 22. The normal coal

contrastingly exhibits a lack of visible pores, even at the higher magnification level used in Figure 23.

The presence of these pores increases the area of interface between the coal and the air. Therefore, the reaction sites in the coal are more readily available to oxygen, increasing the rate of oxidation. The increased oxidation rate implies a higher propensity to self-heat, resulting in the differences observed in each pair of samples. The general relationship is therefore that as a coal becomes more heat-affected, its propensity to self-heat is reduced. However, its propensity to self-heat is higher when compared to a naturally rank advanced coal of a similar rank. In order to fully characterise this relationship, however, further analysis is required.

6.2 KINETIC ANALYSIS

Kinetic analysis investigates the rate at which chemical reactions occur, and was used in order to fully understand the self-heating process. To perform a kinetic analysis, the data was processed to produce Arrhenius-type plots. Figure 24 illustrates a combined Arrhenius plot of all tested samples.

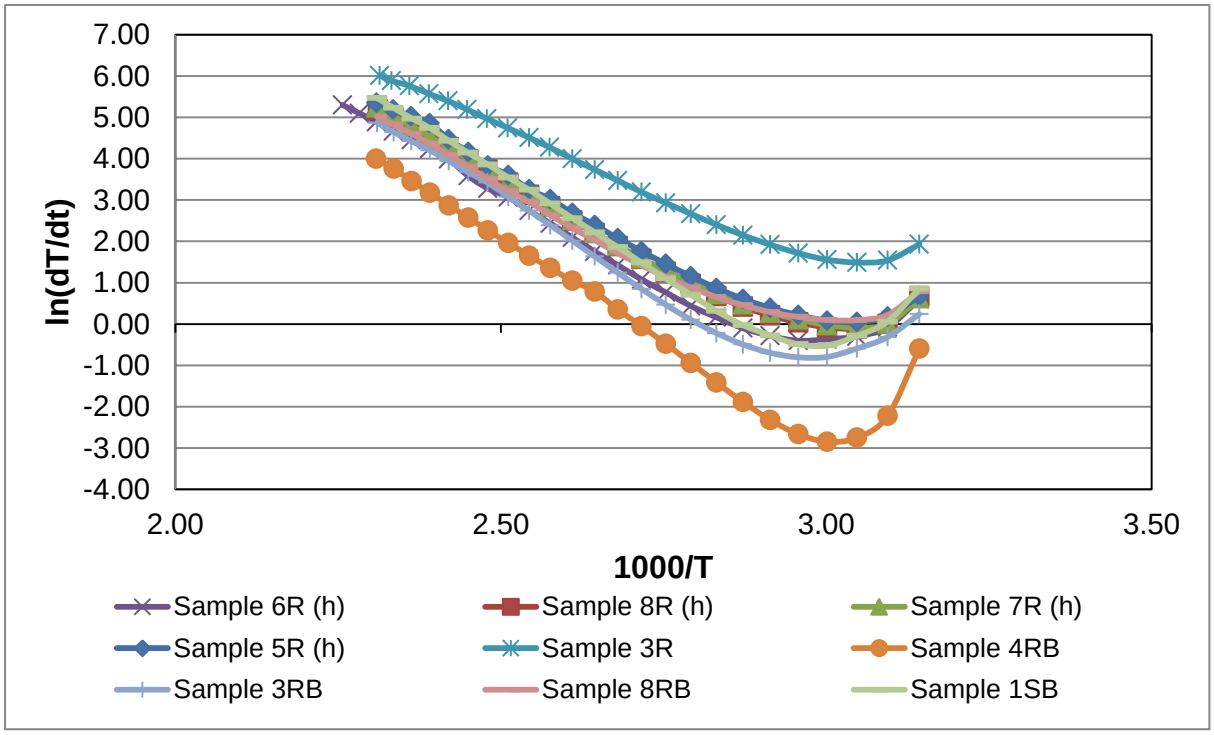

Figure 24. Combined sample Arrhenius plot.

Examining Figure 24, it is clear that the self-heating process occurs in two distinct phases. The first phase occurs at lower temperatures, and is generally characterised by a gradual decrease and then increase in the rate of reaction. This phase is represented in Figure 24 by rightmost, non-linear section of each sample. The second phase occurs at higher temperatures, and is generally characterised by a logarithmically increasing rate of reaction. This phase is represented in Figure 24 by the leftmost, linear section of each sample. The first phase can therefore be described as the non-Arrhenius phase, while the second can be described as the Arrhenius phase.

The non-Arrhenius phase encompasses a range of temperatures from 40°C to beyond 70°C, the extent of which varies with each sample. Because of this, the non-Arrhenius phase is the determining factor in deriving the R_{70} value, and hence an examination of this phase will help in understanding the differences in self-heating behaviour observed in the samples. The Arrhenius phase falls beyond this range of temperatures and thus does not affect the R_{70} value. Investigating this phase will therefore provide further insight into the overall self-heating process.

6.2.1 The Non-Arrhenius Phase

In the analysis of the non-Arrhenius phase, the two pairs of samples of similar rank were compared. These comparisons are given in Figures 25 and 26.

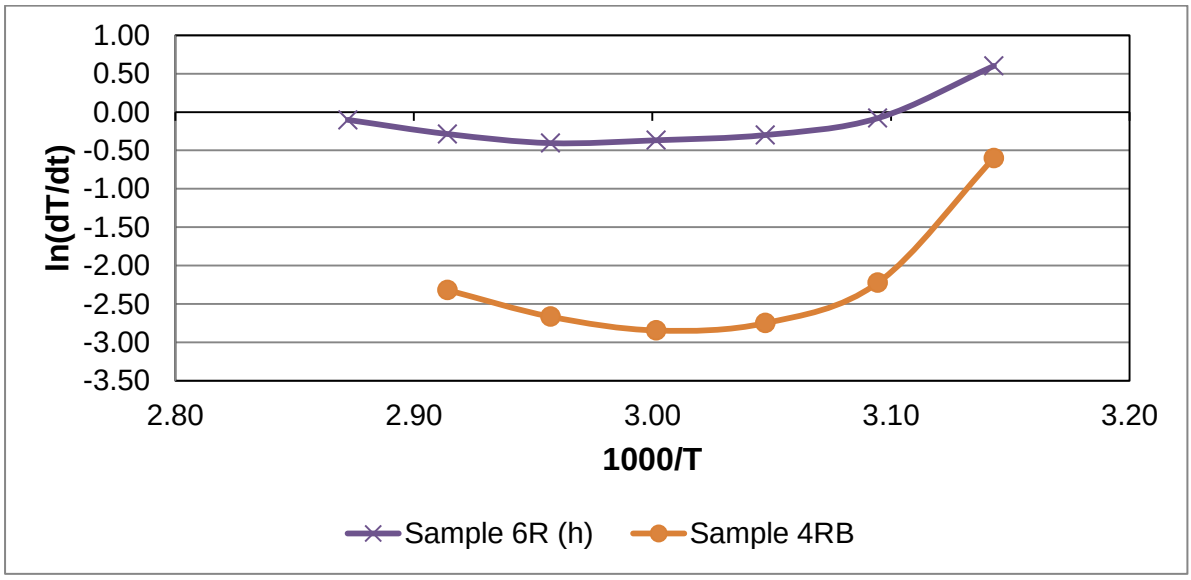

Figure 25. Non-Arrhenius phase comparison of samples 6R and 4RB.

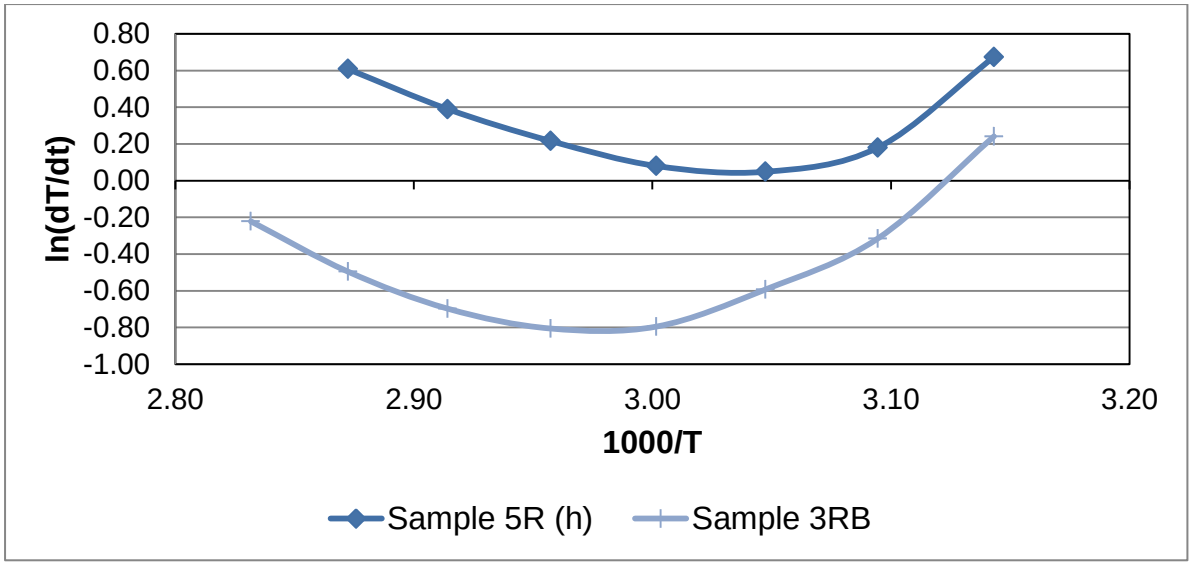

Figure 26. Non-Arrhenius phase comparison of samples 5R and 3RB.

In each of the comparisons the heat-affected coal falls above the normal, with a shallower 'dip' in the curve. Thus the initial slowdown in reaction rate is less intense for the heat-affected coals in comparison to the normal coals. As discussed in Section 6.1, this can be attributed to the relatively larger pore size allowing the oxidation reaction to occur at a faster rate.

6.2.2 The Arrhenius Phase

The Arrhenius phase of each sample is illustrated in Figures 27-35.

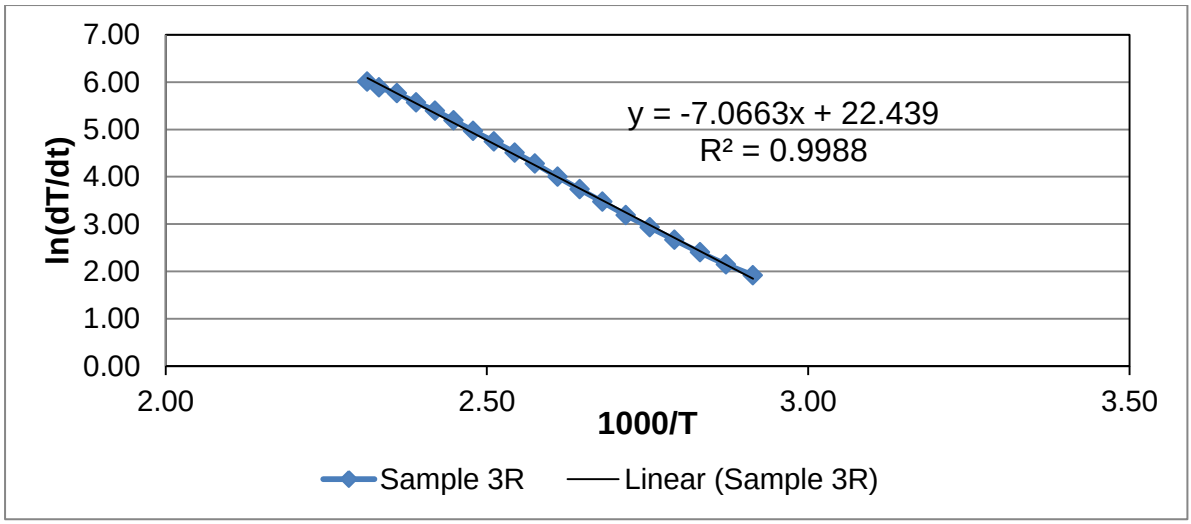

Figure 27. Arrhenius phase of sample 3R.

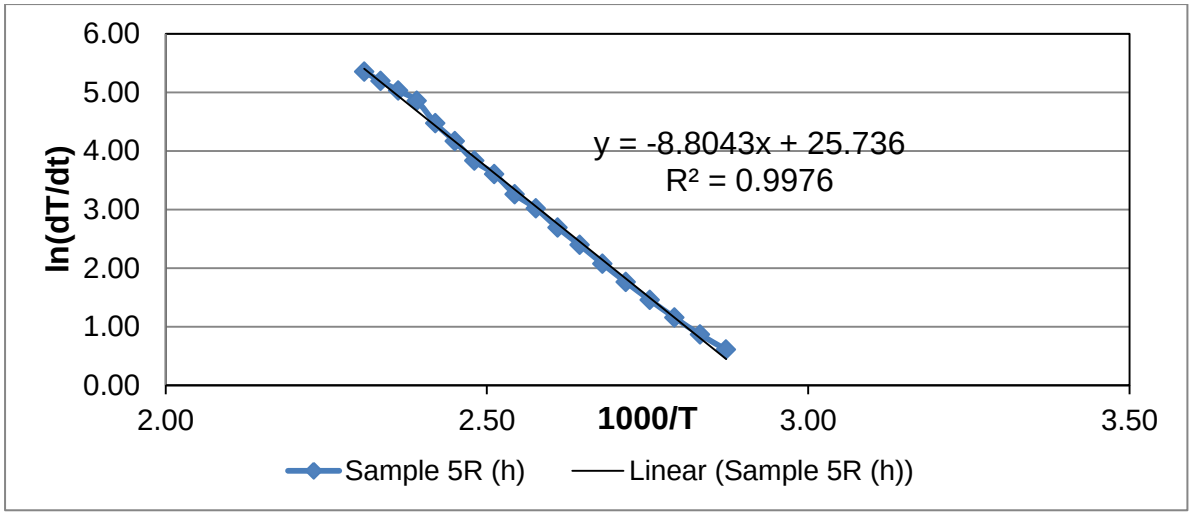

Figure 28. Arrhenius phase of sample 5R.

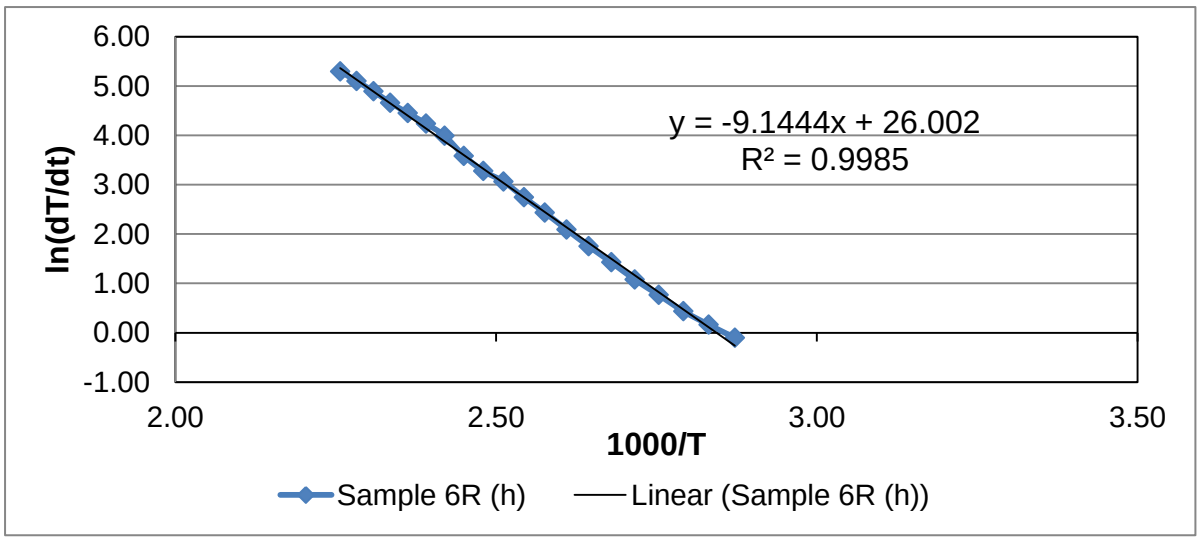

Figure 29. Arrhenius phase of sample 6R

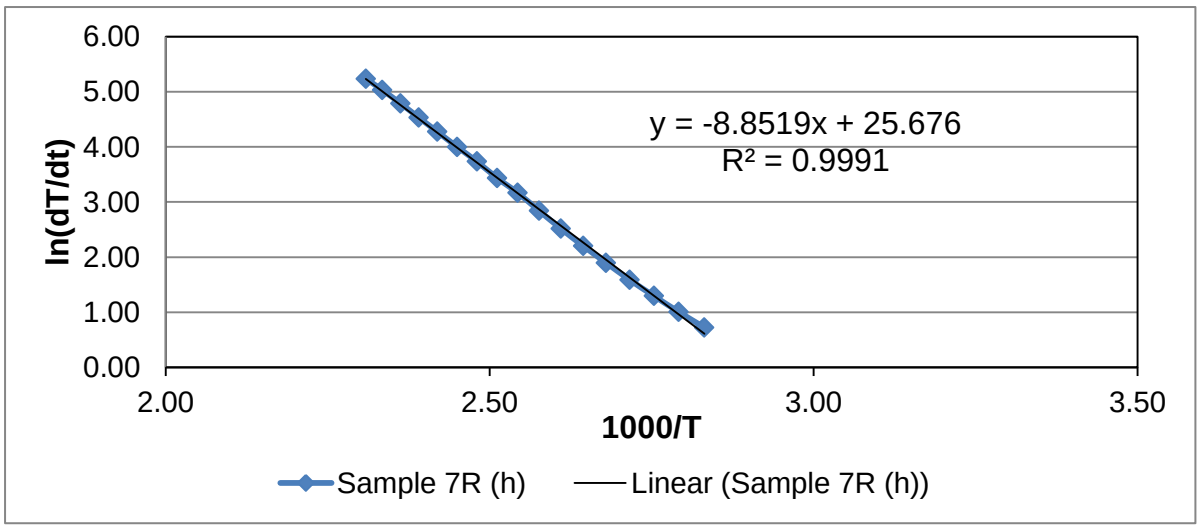

Figure 30. Arrhenius phase of sample 7R.

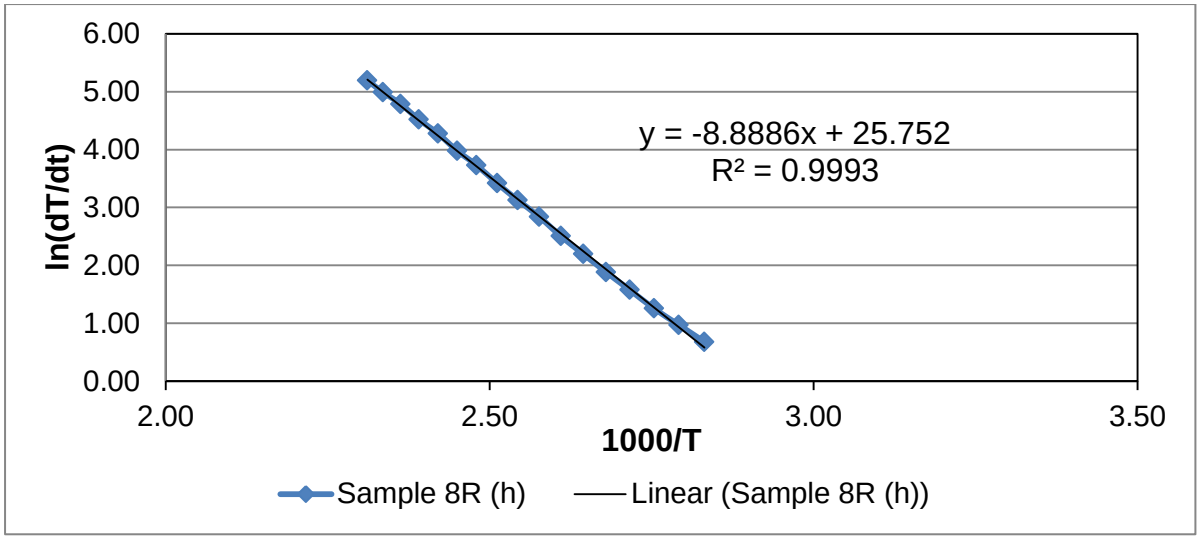

Figure 31. Arrhenius phase of sample 8R.

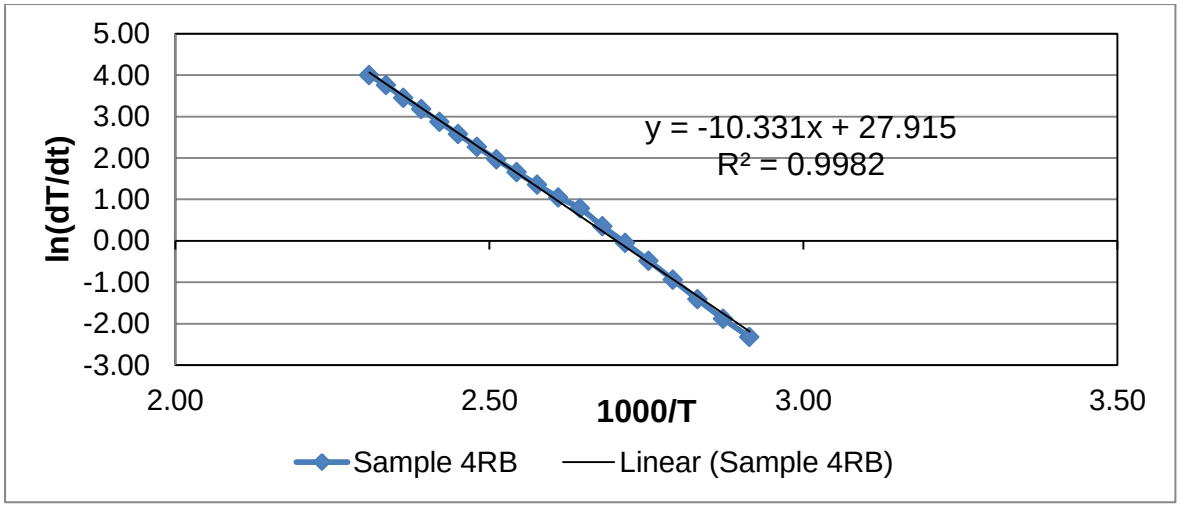

Figure 32. Arrhenius phase of sample 4RB.

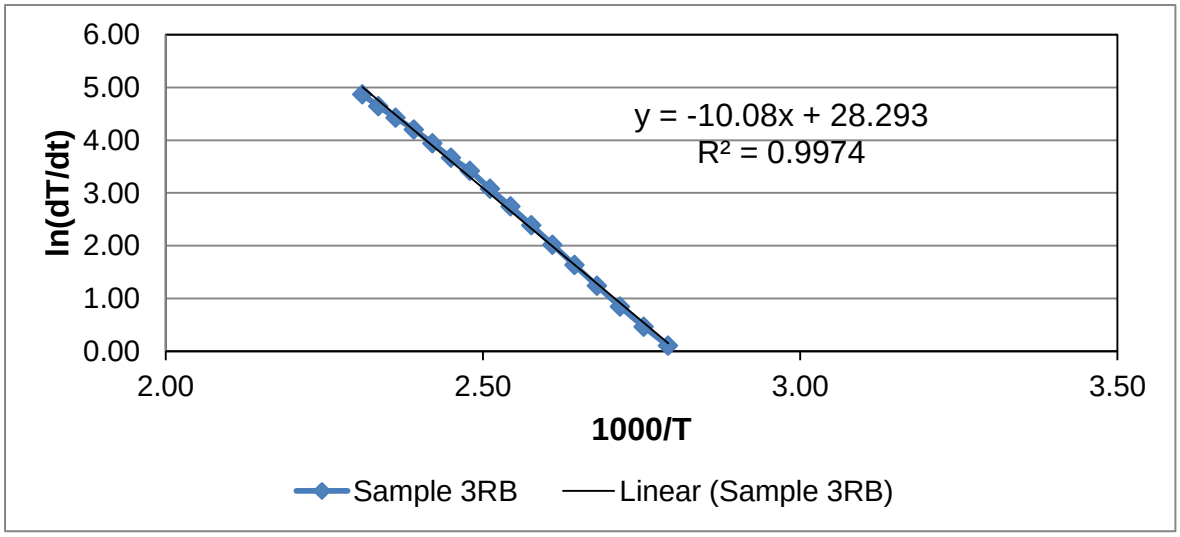

Figure 33. Arrhenius phase of sample 3RB.

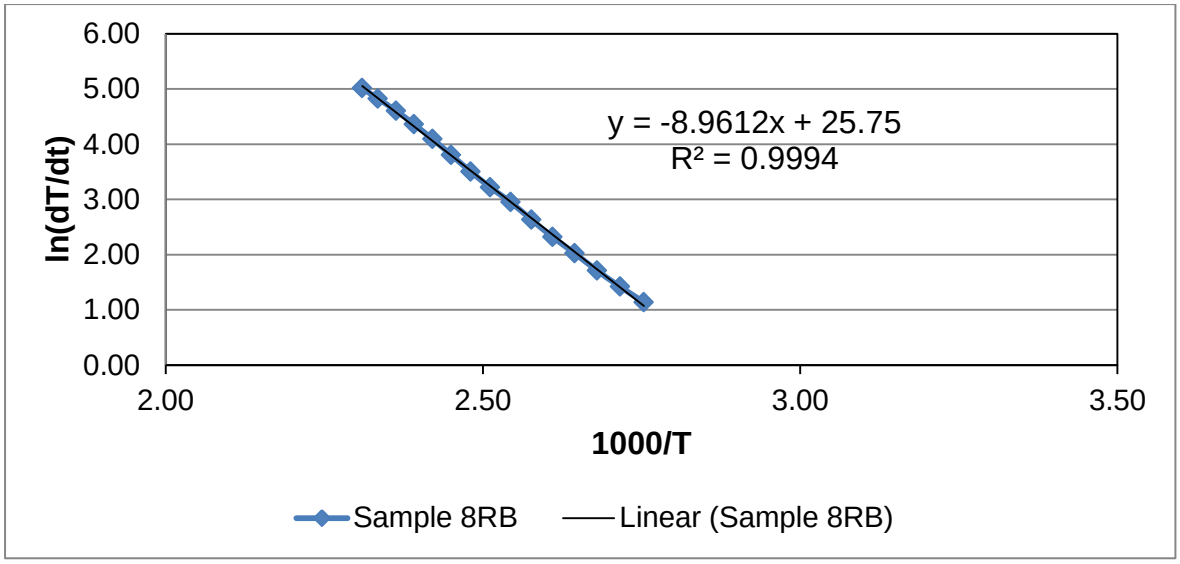

Figure 34. Arrhenius phase of sample 8RB.

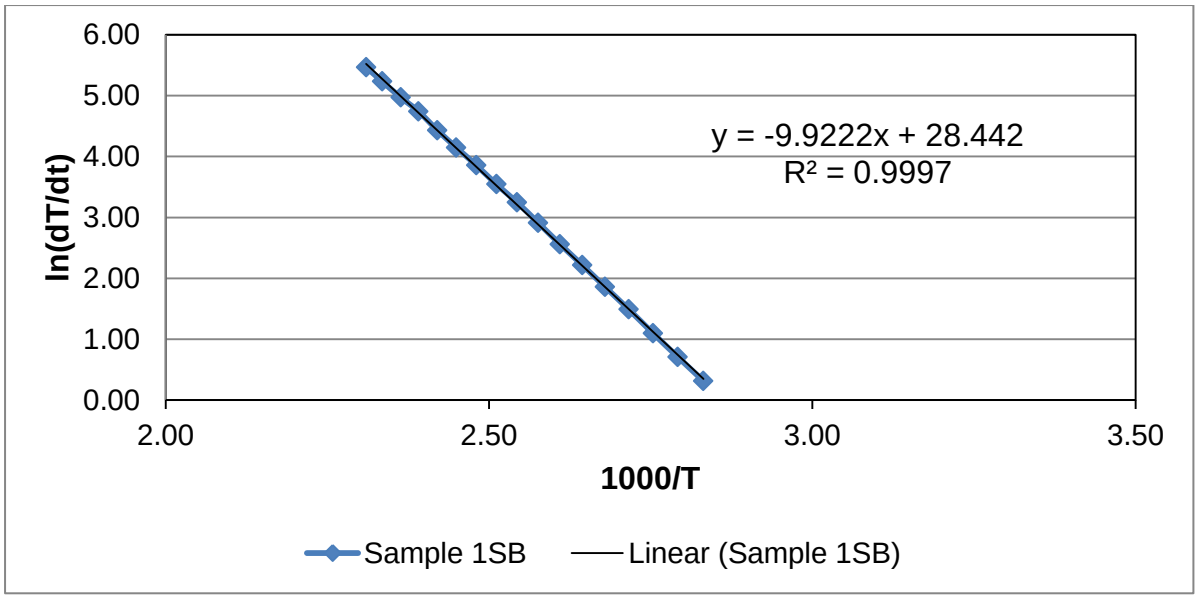

Figure 35. Arrhenius phase of sample 1SB.

Each sample exhibits an extremely high degree of linear correlation, confirming the Arrhenius nature of this phase.

The activation energy, E_a, of each sample can then be calculated from the gradient, m, of the Arrhenius plot, using equation 1, where R is the gas constant.

$$m = \frac{-E_a}{R} \quad (1)$$

A summary of the activation energies of each sample is given in Table 6.

Table 6. Activation energy summary.

Sample ID	E_a (kJ/mol)
3R	58.75
5R (h)	73.20
7R (h)	73.60
8R (h)	73.90
6R (h)	76.03
8RB	74.51
3RB	83.81
4RB	85.90
1SB	82.50

A lower activation energy value indicates that it is easier for the reaction, in this case oxidation, to take place. In order to adequately compare these values, they were plotted against Suggate rank, as given in Figure 36.

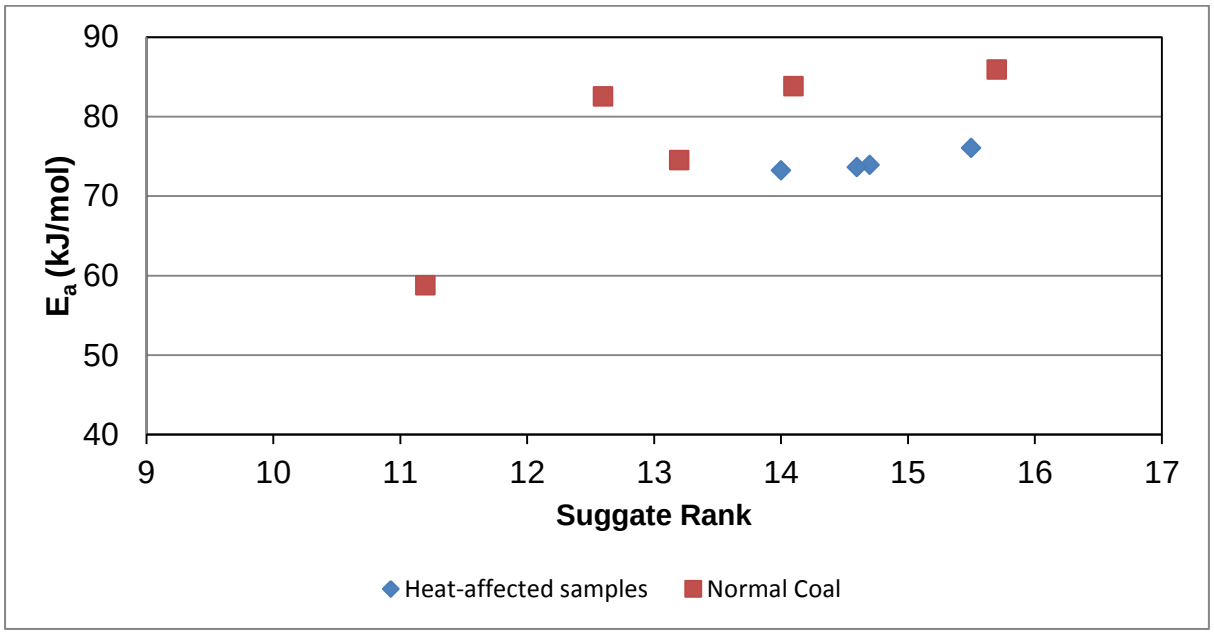

Figure 36. Suggate rank plotted against activation energy for heat-affected and normal samples.

The relationship illustrated in Figure 36 mirrors that observed earlier in Figure 21. The heat-affected coals fall below the normal coals, indicating lower activation energies. The heat-affected coals, however, have higher activation energies when compared to the normal coal from the same site. This reinforces the trend that heat-affected coal is less susceptible to self-heating than the normal coal from which it was formed, yet is more susceptible when compared to normal coal of a similar rank.

A final point of interest is the outlying normal coal sample, 1SB, observed in both Figure 36 and Figure 21, which has a higher activation energy and lower R_{70} value than expected for its rank. With a relatively unremarkable ash content of 4.5%, the underlying reason for this must lie in the physical properties of the sample. A relatively small pore is therefore the most likely cause, inhibiting the ability of the coal to oxidise, thus reducing its propensity to self-heat.

7 IMPLICATIONS FOR HAZARD MANAGEMENT

A lack of understanding of the self-heating properties of heat-affected coal can lead to two mistakes in managing the risk of spontaneous combustion at a site where heat-affected coal occurs, which are:

- A coals propensity to self-heat is overestimated; and
- A coals propensity to self-heat is underestimated.

The first situation could occur where it is not known that a coal is heat-affected, or where the effect of thermal metamorphosis of self-heating properties is not known. In this case, the heat-affected coal might be assumed to have a similar self-heating propensity to the surrounding normal coal. This could result in over-management of the spontaneous combustion risk, incurring unnecessary cost on the operation.

The second situation could occur when a coals susceptibility to self-heating is determined based on its rank. If the formation history of the coal is not known, or the aforementioned effect on self-heating properties is again not known, the coal might be assumed to have a similar self-heating propensity to that of a normal coal of a similar rank. This could result in under-management of the coal, leading to spontaneous combustion and hence the social, environmental and economic risks associated with it.

It is therefore imperative to understand both whether heat-affected coal is present at a site, and its self-heating properties. The presence of heat affected coal should therefore be considered in the creation of a PMHMP, and hence determining the level of spontaneous combustion management required.

Another major factor in spontaneous combustion management is monitoring. The main monitoring method used is the index gases method, which monitors the temperature of the coal based on the gases it emits. The next step in understanding heat-affected coal, therefore, is the investigation of the gases emitted by heat-affected coal in order to determine the variance, if any, from normal coal. This should be undertaken in order to verify the effectiveness of the index gas method of monitoring at sites where heat-affected coal is present.

8 CONCLUSIONS

When a coal becomes heat-affected, its propensity to self-heat is changed. A heat-affected coal will have its propensity to self-heat reduced when compared to the coal from which it was formed. This is attributed to the artificial rank advancement of the coal.

However, when compared to a naturally rank advanced coal of a similar rank, the heat-affected coal will exhibit a higher propensity to self-heat. This is attributed to the mosaic structure of the coal with relatively large, open pores as a result of the lack of pressure component in its formation.

This means that, when assessing the risk of spontaneous combustion, it is important to consider whether coal has been heat-affected, and to what degree, and that simply relying on the coal rank or the surrounding normal coal as an indicator can give misleading results.

Furthermore, coal self-heating cannot be modelled as a simple Arrhenius reaction, but also has a non-Arrhenius phase at low temperatures that forms an integral part of the behaviour.

9 RECOMMENDATIONS

Based on the findings of this study, the following recommendations are made:

- In the assessment of spontaneous combustion risk as part of a PMHMP, the presence of heat-affected coal is an important factor. Heat-affected areas of coal should therefore undergo testing to determine their propensity to self-heat in order to provide an adequate PMHMP;
- In the simulation modelling of coal self-heating as a means to predict spontaneous combustion, the changed self-heating properties of heat-affected coal should be accurately reflected in the resulting model;
- In the study of the process of coal self-heating, the low temperature non-Arrhenius phase of the reaction should be considered and warrants further in-depth investigation; and
- In the further study of the self-heating of heat-affected coal, the resultant gases released should be examined in order to verify the accuracy of current monitoring methods.

7 REFERENCES

Arisoy, A and Beamish, B, 2008. Effect of intrinsic coal properties on self-heating rates, in *Proceedings 12th US/North American Mine Ventilation Symposium* (Ed: K G Wallace Jr), pp 149-153 (The Society of Mining, Metallurgy and Exploration Inc, Littleton, USA)

Arisoy, A and Beamish, B, 2015. Mutual effects of pyrite and moisture on coal self-heating rates and reaction rate data for pyrite oxidation, *Fuel*, 139:107-114.

Arisoy, A and Beamish, B, 2015. Reaction kinetics of coal oxidation at low temperatures, *Fuel*, 159:412-417.

Beamish, B B and Blazak, D G, 2005. Relationship between ash content and R70 self-heating rate of Callide Coal, International Journal of Coal Geology, *64(1-2):126-132.*

Beamish, B B and Hamilton, G R, 2005. Effect of moisture content on the R70 self-heating rate of Callide coal, *International Journal of Coal Geology*, 64(102):133-138.

Beamish, B B, Barakat, D G and St George, J D, 2000. Adiabatic testing procedures for determining the self-heating propensity of coal and sample ageing effects, *Thermochimica Acta*, 362(1-2): 79-87.

Beamish, B B, Blazak D G, Hogarth L C S, and Jabouri I, 2005. R70 relationships and their interpretation at a mine site, in *Proceedings of 2005 Coal Operators Conference* (Ed: N Aziz), pp 103-186 (University of Wollongong & the Australasian Institute of Mining and Metallurgy).

Beamish, B, 2016. Personal communication, Associate Professor, University of Queensland School of Mining Engineering, 16th September.

Beamish, B, 2005. Comparison of the R70 self-heating rate of New Zealand and Australian coals to Suggate rank parameter, *International Journal of Coal Geology*, 64(1-2):139-144.

Beamish, B, Cosgrove, M and Theiler, J, 2016. Self-heating behaviour of heat-affected coal, in (Ed: N Aziz), pp 451-455 (University of Wollongong & the Australasian Institute of Mining and Metallurgy).

Carras, J N, Day, S, Saghafi, A and Roberts, O C, 2009. Spontaneous cobustion in open cut coal mines - recent Australian research, in *Proceedings of 2005 Coal Operators Conference* (Ed: N Aziz), pp 195-200 (University of Wollongong & the Australasian Institute of Mining and Metallurgy).

Cliff, D, Brady, D and Watkinson, M, 2014. Developments in the management of spontaneous combustion in Australian underground coal mines, in *Proceedings of 2014 Coal*

Operators Conference (Ed: N Aziz), pp 330-338 (University of Wollongong & the Australasian Institute of Mining and Metallurgy).

Deng, J, Ma, X, Zhang, Li, Y and Zhu, W, 2015. Effects of pyrite on the spontaneous combustion of coal, *International Journal of Coal Science & Technology,* 2(4):306-311.

Dudzinska, A, 2014.The effect of pore volume of hard coals on their susceptibility to spontaneous combustion, *Journal of Chemistry*, 2014(3):1-7.

Fredericks, P M, Warbrooke P and Wilson, M A, 1985. A study of the effect of igneous intrusions on the structure of an Australian high volatile bituminous coal, Organic Geochemistry, 8(5):329-340.

Jones, J C and Newman, S C, 2003. Non-Arrhenius behaviour in the oxidation of two carbonaceous substrates, Journal of Loss Prevention in the Process Industry, *16(3):223-225.*

Kam, A Y, Hixson, A N and Perlmutter, D D, 1976. The oxidation of bituminous coal – I: Development of a mathematical model, *Chemical Engineering Science,* 31(9):815-819.

Kaymakci, E and Didari, V, 2002. Relations between coal properties and spontaneous combustion parameters, *Journal of Engineering & Environmental Sciences,* 26(1):59-64.

Kucuk, A, Kadioglu, Y and Gulaboglu, M S, 2003. A study of spontaneous combustion characteristics of a Turkish lignite: particle size, moisture of coal, humidity of air, *Combustion and Flame,* 133(3):255-261.

Kwiecinska, B, and Petersen, H I, 2004. Graphite, semi-graphite, natural coke and natural char classification - ICCP system, *International Journal of Coal Geology*, 57(2):99-116

Mohalik, N, Panigrahi, D, Singh, V and Singh, R, 2009. Assessment of spontaneous heating of coal by differential scanning calorimetric technique – an overview, in *Proceedings of 2009 Coal Operators Conference* (Ed: N Aziz), pp 303-310 (University of Wollongong & the Australasian Institute of Mining and Metallurgy).

Nalbandian, H, 2010. Propensity of coal to self heat [online]. Available from <www.usea.org/sites/default/files/102010_Propensity%20of%20coal%20to%20self-heat_ccc172.pdf> [Accessed: 24 May 2016]

Qi, X, Xue, H, Xin, H, and Wei, C, 2016. Reaction pathways of hydroxyl groups during coal spontaneous combustion, *Canadian Journal of Chemistry,* 94(5):494-500.

Ray, S K and Panigrahi, D C, 2015. Recent development in determining the spontaneous heating susceptibility of Indian coals and its correlation with intrinsic parameters of coal, *Journal of The Institution of Engineers (India),* 96(2):159-167.

Rimmer, S M, Yoksoulian, L E and Hower, J C, 2009. Anatomy of an intruded coal, I: Effect of contact metamorphism on whole-coal geochemistry, Springfield (No. 5) (Pennsylvanian) coal, Illinois Basin, *International Journal of Coal Geology*, 79(3):74-82.

Roberts, F I, Warbrooke, P R, Ward, C R, 1989. Geochemical and mineralogical changes in a coal seam due to contact metamorphism, Sydney Basin, New South Wales, Australia, *International Journal of Coal Geology,* 11(2):105-125.

Singh, A K, Sharma, M and Singh, M P, 2008. Genesis of natural cokes: some Indian examples, *International Journal of Coal Geology*, 75(1):40-48.

Singh, A K, Singh, M P, Sharma, M and Srivastava, S K, 2007. Microstructures and microtextures of natural cokes: A case study of heat-affected coking coals from the Jharia coalfield, India, *International Journal of Coal Geology,* 71(2-3):153-175.

Singh, R V K, 2013. Spontaneous heating and fire in coal mines, *Procedia Engineering,* 62:78-90.

Southern Illinois University, 2016. Coal Macerals Scroll | Petrographic Atlas [Online]. Available from <http://coalandcarbonatlas.siu.edu/coal-macerals/scroll.php> [Accessed 26th September, 2016]

Stracher, G B, 2007. *Geology of Coal Fires: Case Studies From Around the World,* pp 62-70 (Geological Society of America: Boulder,Colorado)

Stracher, G B, 2010. *Coal and Peat Fires: A Global Perspective: Volume 1: Coal – Geology and Combustion*, pp 115-125 (Elsevier Science: United Kingdom).

Suggate, R P, 2000. The Rank(Sr) scale: Its basis and its applicability as a maturity index for all coals, *New Zealand Journal of Geology and Geophysics*, 43(4):521-553.

Taylor, G H, Teichmuller, M, Davis, A, Diessel, C F K, Littke, R, Robert, P, 1998. *Organic Petrology*, pp 704 (Gebruder Borntraeger, Berlin-Stuttgart).

Wang, H, Dlugogorski, B Z and Kennedy, E M, 2003b. Analysis of the mechanism of the low-temperature oxidation of coal, *Combustion and Flame*, 134(1–2):107-117.

Wang, H, Dlugogorski, B Z, Kennedy, E M, 2003a. Coal oxidation at low temperatures: oxygen consumption, reaction mechanism and kinetic modelling, *Progress in Energy and Combustion Science,* 29(6):487-513.

Wang, X, 2014. Experimental and Theoretical Studies of Kinetics and Quality Parameters to Determine Spontaneous Combustion Propensity of U.S. Coals, PhD thesis, West Virginia University, Morgantown.

Xie, J, Xue, S, Cheng, W and Wang, G, 2011. Early detection of spontaneous combustion of coal in underground coal mines with development of an ethylene enriching system, *International Journal of Coal Geology,* 85(1):123-127.

Xu, T, Wang, D, and He, Q, 2013. The study of the critical moisture content at which coal has the most high tendency to spontaneous combustion, *International Journal of Coal Preparation and Utilization,* 33(3):117.

Xuyao, Q, Wang, D, Milke, J A and Zhong, X, 2011. Crossing point temperature of coal, *Mining Science and Technology (China),* 21(2):255-260.

Yao, Y, Liu, D and Huang, W, 2011. Influences of igneous intrusions on coal rank, coal quality and adsorption capacity in Hongyang, Handan and Huaibei coal fields, North China, *International Journal of Coal Geology,* 88(2-3):135-146.

Yuan, L and Smith, A C, 2012. The effect of ventilation on spontaneous heating of coal, *Journal of Loss Prevention in the Process Industry,* 25(1):131-137.

Zhang, H, Gao, E and Zhang, X, 2015. Comprehensive study on bituminous coal oxidation by TGA-DTA-FTIR experiment, *Journal of Power Technologies,* 95(3):167-174.

8 APPENDIX A – PROXIMATE ANALYSIS DATA

Sample ID	Moisture (%)	Ash Content (%)	Volatile Matter (%)	Fixed Carbon (%)	Sulphur	Calorific Value	Reflectance (O_{daf})	Volatile Matter (dmmsf)	Calorific Value (dmmsf)
5R (h)	1.6	2.9	30.4	65.1	0.71	34.19	6.1	31.1	15524
7R (h)	1.5	4.8	24.8	68.9	0.74	33.54	4.3	25.5	15559
8R (h)	1.5	6.6	24.1	67.8	0.89	32.99	4.3	25.0	15658
6R (h)	1.5	9.3	20.0	69.2	1.11	32.09	3.0	20.6	15777
3R	3.9	1.6	39.0	55.5	0.59	32.07	9.6	40.8	14681
8RB	2.0	16.6	30.4	51.0	0.61	28.30	8.0	35.5	15344
3RB	1.6	4.9	28.8	64.7	0.35	33.56	5.0	30.2	15555
4RB	0.8	12.7	18.0	68.5	0.37	30.90	4.4	19.3	15636
1SB	1.7	4.5	36.6	57.2	0.61	33.19	6.4	38.3	15359

9 APPENDIX B – RAW ADIABATIC TESTING DATA

Table 7. Sample 3R raw adiabatic data.

Coal Temp (^{o}C)	Time (min)	Time (h)
39.9	0	0.00
45.0	44.50	0.74
50.0	108.83	1.81
55.0	176.50	2.94
60.0	239.83	4.00
65.0	293.83	4.90
70.0	337.83	5.63
75.0	372.83	6.21
80.0	400.00	6.67
85.0	420.83	7.01
90.0	436.83	7.28
95.0	449.17	7.49
100.0	458.50	7.64
105.0	465.67	7.76
110.0	471.17	7.85
115.2	475.50	7.92
120.0	478.67	7.98
125.1	481.33	8.02
130.3	483.50	8.06
135.3	485.17	8.09
140.2	486.50	8.11
145.3	487.67	8.13
150.6	488.67	8.14
155.6	489.50	8.16
159.0	490.00	8.17

Table 8. Sample 5R raw adiabatic data.

Coal Temp (^{o}C)	Time (min)	Time (h)
40.2	0	0.00
45.0	146.83	2.45
50.0	397.33	6.62
55.0	683.17	11.39
60.0	960.17	16.00
65.0	1201.83	20.03
70.0	1405.00	23.42
75.0	1568.33	26.14
80.0	1694.33	28.24
85.0	1788.83	29.81
90.0	1858.83	30.98
95.0	1910.33	31.84
100.0	1948.00	32.47
105.0	1975.33	32.92
110.0	1995.67	33.26
115.0	2010.33	33.51
120.0	2021.83	33.70
125.0	2030.00	33.83
130.0	2036.50	33.94
135.0	2041.17	34.02
140.1	2044.67	34.08
145.1	2047.00	34.12
150.2	2049.00	34.15
155.2	2050.67	34.18

Table 9. Sample 6R raw adiabatic data.

Coal Temp (^{o}C)	Time (min)	Time (h)
39.9	0	0.00
45.0	167.67	2.79
50.0	492.33	8.21
55.0	897.00	14.95
60.0	1330.17	22.17
65.0	1779.83	29.66
70.0	2179.33	36.32
75.0	2511.50	41.86
80.0	2766.67	46.11
85.0	2960.67	49.34
90.0	3100.33	51.67
95.0	3202.50	53.38
100.0	3274.67	54.58
105.0	3326.67	55.44
110.0	3363.67	56.06
115.0	3390.00	56.50
120.0	3409.33	56.82
125.0	3423.33	57.06
130.0	3434.67	57.24
135.0	3443.00	57.38
140.1	3448.67	57.48
145.1	3453.00	57.55
150.1	3456.50	57.61
155.1	3459.33	57.66
159.9	3461.50	57.69
164.9	3463.33	57.72
169.9	3464.83	57.75

Table 10. Sample 7R raw adiabatic data.

Coal Temp (^{o}C)	Time (min)	Time (h)
40.4	0	0.00
45.0	148.67	2.48
50.0	446.67	7.44
55.0	773.83	12.90
60.0	1082.50	18.04
65.0	1351.33	22.52
70.0	1579.67	26.33
75.0	1766.67	29.44
80.0	1912.33	31.87
85.0	2022.17	33.70
90.0	2104.33	35.07
95.0	2165.67	36.09
100.0	2210.67	36.84
105.0	2243.83	37.40
110.0	2268.00	37.80
115.0	2285.50	38.09
120.0	2298.17	38.30
125.0	2307.83	38.46
130.0	2315.00	38.58
135.0	2320.50	38.67
140.2	2324.83	38.75
145.1	2328.00	38.80
150.1	2330.50	38.84
155.2	2332.50	38.88
159.9	2334.00	38.90

Table 11. Sample 8R raw adiabatic data.

Coal Temp (^{o}C)	Time (min)	Time (h)
40.0	0	0.00
45.0	154.83	2.58
50.0	454.33	7.57
55.0	790.17	13.17
60.0	1115.17	18.59
65.0	1403.67	23.39
70.0	1647.50	27.46
75.0	1845.33	30.76
80.0	1997.50	33.29
85.0	2111.00	35.18
90.0	2196.50	36.61
95.0	2258.50	37.64
100.0	2304.17	38.40
105.0	2337.50	38.96
110.0	2362.00	39.37
115.0	2379.50	39.66
120.0	2392.67	39.88
125.0	2402.50	40.04
130.1	2409.83	40.16
135.0	2415.33	40.26
140.0	2419.50	40.32
145.1	2422.83	40.38
150.1	2425.33	40.42
155.0	2427.33	40.46
159.5	2428.83	40.48

Table 12. Sample 4RB raw adiabatic data.

Coal Temp (^{o}C)	Time (min)	Time (h)
39.8	0	0.00
45.0	567.50	9.46
50.0	3338.59	55.64
55.0	8031.58	133.86
60.0	13198.30	219.97
65.0	17514.33	291.91
70.0	20569.16	342.82
75.0	22547.64	375.79
80.0	23782.59	396.38
85.0	24550.70	409.18
90.0	25036.33	417.27
95.0	25351.66	422.53
100.0	25562.73	426.05
105.0	25699.56	428.33
110.0	25804.89	430.08
115.0	25882.39	431.37
120.0	25939.73	432.33
125.0	25981.89	433.03
130.0	26013.06	433.55
135.0	26035.89	433.93
140.0	26052.89	434.21
145.0	26065.39	434.42
150.0	26074.89	434.58
155.0	26081.89	434.70
160.0	26087.39	434.79

Table 13. Sample 8RB raw adiabatic data.

Coal Temp (^{o}C)	Time (min)	Time (h)
40.0	0	0.00
45.0	135.50	2.26
50.0	376.00	6.27
55.0	648.83	10.81
60.0	921.83	15.36
65.0	1174.50	19.57
70.0	1399.50	23.32
75.0	1589.67	26.49
80.0	1746.17	29.10
85.0	1870.50	31.17
90.0	1966.50	32.77
95.0	2039.00	33.98
100.0	2093.17	34.89
105.0	2132.67	35.54
110.0	2162.17	36.04
115.0	2183.67	36.39
120.0	2199.33	36.66
125.0	2211.33	36.86
130.0	2220.33	37.01
135.0	2227.00	37.12
140.0	2232.00	37.20
145.0	2235.83	37.26
150.0	2238.83	37.31
155.2	2241.33	37.36
159.8	2243.17	37.39

Table 14. Sample 3RB raw adiabatic data.

Coal Temp (^{o}C)	Time (min)	Time (h)
39.9	0	0.00
45.0	240.50	4.01
50.0	651.50	10.86
55.0	1194.33	19.91
60.0	1858.77	30.98
65.0	2530.25	42.17
70.0	3132.91	52.22
75.0	3625.35	60.42
80.0	3999.88	66.66
85.0	4270.23	71.17
90.0	4458.58	74.31
95.0	4587.03	76.45
100.0	4673.80	77.90
105.0	4732.42	78.87
110.0	4772.32	79.54
115.0	4799.84	80.00
120.0	4819.16	80.32
125.0	4833.00	80.55
130.1	4843.00	80.72
135.0	4850.50	80.84
140.0	4856.33	80.94
145.0	4860.83	81.01
150.1	4864.50	81.07
155.0	4867.33	81.12
159.7	4869.50	81.16

Table 15. Sample 1SB raw adiabatic data.

Coal Temp (^{o}C)	Time (min)	Time (h)
40.2	0	0.00
45.0	121.67	2.03
50.0	404.50	6.74
55.0	804.33	13.41
60.0	1308.83	21.81
65.0	1798.00	29.97
70.0	2193.33	36.56
75.0	2502.17	41.70
80.0	2721.00	45.35
85.0	2868.67	47.81
90.0	2968.67	49.48
95.0	3036.33	50.61
100.0	3083.17	51.39
105.0	3115.83	51.93
110.0	3139.00	52.32
115.0	3155.33	52.59
120.0	3167.00	52.78
125.0	3175.67	52.93
130.0	3182.00	53.03
135.1	3186.83	53.11
140.0	3190.33	53.17
145.1	3193.00	53.22
149.9	3195.00	53.25
155.1	3196.67	53.28
159.7	3197.83	53.30